

## Simulating river regulation and reservoir performance in a continental-scale hydrologic model

A.A.G. Tefs<sup>a,b,\*</sup>, T.A. Stadnyk<sup>a,b</sup>, K.A. Koenig<sup>c</sup>, S.J. Déry<sup>a,d</sup>, M.K. MacDonald<sup>a</sup>, P. Slota<sup>c</sup>, J. Crawford<sup>c</sup>, M. Hamilton<sup>a</sup>

<sup>a</sup> Department of Civil Engineering, University of Manitoba, Winnipeg, R3T 5V6, MB, Canada

<sup>b</sup> Department of Geography, University of Calgary, Calgary, AB, T2N 1N4, Canada

<sup>c</sup> Water Resources Engineering Division, Manitoba Hydro, Winnipeg, MB, R3C 0G8, Canada

<sup>d</sup> Environmental Science and Engineering Program, University of Northern British Columbia, Prince George, BC, V2N 4Z9, Canada



### ARTICLE INFO

#### Keywords:

Hydrologic modelling  
Hydroelectric regulation  
Hudson bay

### ABSTRACT

This study develops a novel reservoir regulation routine, incorporated into a continental-scale hydrologic model in the Nelson, Churchill, Yenisey, Ob, and Lena basins. This regulation routine is integrated into the Hydrological Predictions for the Environment (HYPE) hydrologic model, used for continental-scale applications. Applying this daily timestep regulation routine at 19 reservoirs in the Arctic Ocean watershed, performance is shown to improve upon the reservoir regulation currently available in the HYPE model when testing outflow and storage Nash Sutcliffe Efficiencies (NSEs). Improvements stem from intra-annually variable storage rule curves and a variety of stage-dependent outflow functions, improving simulation skill (median NSE increases of 0.18 over 21 reservoir outflow records and 0.49 over 19 reservoir storage records). This new, reservoir regulation routine is suitable for continental-scale modelling by deriving varying, rather than fixed, threshold water surface levels and associated outflow rules in a programmatic way for multiple reservoirs.

### Software and data availability

HYPE: Access to the Hydrologic Predictions for the Environment (HYPE) and Hydrologic Simulation System (HYSS) model codes was granted by the Swedish Meteorological and Hydrologic Institute (SMHI). Details can be found at: <https://sourceforge.net/projects/hype/>.

Microsoft Excel: A commercially available spreadsheet interface tool, available with the Microsoft Office suite of products.

R: Rstudio has been used to develop code for estimating reservoir parameters, simulating reservoir outflow and storage, analyzing simulated data, and plotting results.

Data: Input data used in modelling for reference/calibration/validation are freely available. These are obtained from the Water Survey of Canada (WSC; <https://wateroffice.ec.gc.ca>), the Global Runoff Data Centre (GRDC; <https://portal.grdc.bafg.de>), and the Global Reservoir and Lake Monitoring program (G-REALM; [https://ipad.fas.usda.gov/cropexplorer/global\\_reservoir/](https://ipad.fas.usda.gov/cropexplorer/global_reservoir/)).

### 1. Introduction

In a world increasingly affected by anthropogenic effects, it is natural that interest in modelling of damming and reservoir regulation on streamflow would grow alongside increased resolution and scale in hydrologic modelling. Reservoir regulation exists as an optional extension (to some degree of sophistication) in most hydrologic models (Nazemi & Wheater, 2015a, 2015b). Modelling of reservoir regulation is most straightforwardly seen in basin-scale studies, such as those, where regulation has been shown to improve operational modelling (Piman et al., 2016; Ahn et al., 2014). A practical combination of hydrologic and reservoir modelling is seen in a Canada-wide study of climate change's effect on hydroelectric production looking to develop empirical relationships between historical climatology and hydroelectric production, then projecting these results to a possible future climate (Amir Jabbari and Nazemi, 2019). This study cites Manitoba and Saskatchewan (studied extensively here) as difficult-to-predict areas due to their streamflow largely originating far upstream of regulation points and having high interannual variability. A reasonable solution to this

\* Corresponding author. 2500 University Drive NW, University of Calgary, Calgary, AB, T2N 1N4, Canada.

E-mail address: [andrew.tefs@ucalgary.ca](mailto:andrew.tefs@ucalgary.ca) (A.A.G. Tefs).

problem is the full integration of hydrologic and reservoir regulation modelling at the watershed or continental scale, covering numerous reservoirs simultaneously.

As computational hydrology has grown to include continental-scale studies, so too has interest in regulation's effects on continental or global hydrology (Qin et al., 2019) and modelling to simulate anthropogenic impacts and climate change, with varying degrees of success (Yassin et al., 2019; Coerver et al., 2018; Arheimer et al., 2017; Zajac et al., 2017; Bellin et al., 2016; Zhao et al., 2016; Pechlivanidis and Arheimer, 2015; Zhou and Guo, 2013; Pokhrel et al., 2012). The Hydrological Predictions for the Environment (HYPE; Lindström et al., 2010) model is proven to be useful for simulating hydrology at the continental-scale (Pechlivanidis and Arheimer, 2015), but the regulation algorithm can be problematic at that scale, due to the need to calibrate reservoir parameters separately from autocalibration. This routine has been indirectly evaluated and found to be poorly represented at larger scales and/or in data-sparse regions (Arheimer et al., 2020; Donnelly et al., 2014, 2016; Andersson et al., 2015; Bergstrand et al., 2013). Human-water interactions (reservoir management, irrigation, etc.) are also noted as a problem-area in other continental-scale hydrologic models and global land surface models (Zaherpour et al., 2018; Wada et al., 2017; Wanders and Wada, 2015; Zhou and Guo, 2013; Pokhrel et al., 2012; Hanasaki et al., 2006). A useful survey of the representation of human-water-interactions in macroscale hydrologic models can be found Nazemi and Wheater (2015a). With regulation of reservoirs implemented into large-scale hydrologic modelling, studies of sensitivity, uncertainty, or the effects of climate change at the continental scale become possible.

Studies have created reservoir regulation site-specific models developed to be integrated directly into larger hydrological models (Alvarez et al., 2014; Welsh et al., 2013; Li et al., 2010a; Minville et al., 2010; Minville et al., 2009a). Many studies are developed using historical data and applied to overtly non-stationary future climates using dynamically or stochastically optimized methods (Denaro et al., 2017; Haguma et al., 2014a,b; Haguma et al., 2014a,b; Malekmohammadi et al., 2009). Other Canada-based studies have used future climatic ensembles and current reservoir operations rules as the work presented in this paper will, but instead to analyse reservoir reliability, sensitivity, or uncertainty (Hassanzadeh et al., 2014; Li et al., 2010; Minville et al., 2009b) as this work will not. An important development in the rarefaction of regulation modelling is accounting for intra-annual changes to operations (due to ice-cover, inflow regime, or hydroelectric demand). Operational rule curves (or optimal release curves based on storage) with hedging, or with curves optimized dynamically have been validated on historical periods and proposed for operational use (Prasanchum and Kangrang, 2018; Zhang et al., 2017; Nunes et al., 2016; Adeloye et al., 2015; Taghian et al., 2013; Liu et al., 2011; Matrosov et al., 2011) an example of the utility of intra-annually variable target storage curves is presented in this work in the context of basins with variable interannual (climatic variability) and intra-annual (nival regime) inflow.

The effects of future climate change and changing inflow regimes are sure to pass on to reservoir operations. The cumulative future effects of regulation and climate change are of growing concern. The climate is changing rapidly in northern Canada (Déry et al., 2009, 2011) leading to changes in the duration and depth of snowpacks (Kang et al., 2014), and ultimately resulting in alteration of both the timing and volume of freshwater export to the Arctic Ocean. At the same time, regulation control over freshwater exports, for example to the Hudson Bay Complex from the Nelson-Churchill River Basin (NCRB) and La Grande Rivière Complex (LGRC), have been increasing through time, influencing the timing and volume of freshwater exports (Déry et al., 2016, 2018). The confluence of the effects of regulation and climate change on Hudson Bay triggered the onset of the BaySys group of projects (Barber, 2014), designed to examine the full extent of these impacts on the marine system of Hudson Bay. Of interest is the question: "Is climate change or

hydroelectric regulation the primary driver of changes in Hudson Bay?". To determine the answer, the effects of both drivers must be quantifiably simulated, separated, and analysed. Models used to project future terrestrial freshwater exports must be robust in changing climates, reliable for long-term projections in cold regions, and responsive to changing or variable inflow conditions to regulated reservoirs, which is often not the case in currently existing hydrological models. The Hudson Bay Drainage Basin (HBDB) and those rivers draining to the Arctic Ocean as a whole contain multiple regulation points (reservoirs, control structures, generating stations, diversions, etc.), with close to half of the freshwater of the HBDB (by volume) impacted by regulation (Déry et al., 2018) and the impact of regulation on environmental factors of note in the Yakutia region of Russia (Tyaptirgyanov and Tyaptirgyanova, 2016; Crate, 2002).

The Freshwater Systems group (Team 2) of BaySys (Barber, 2014) is tasked with generating two hydrologic models to simulate an ensemble of climate scenarios: (1) a regulated system model and (2) a re-naturalized model. To do so, an improved reservoir routine embedded in HYPE is necessary. It must effectively simulate reservoir outflows under natural climatic variability (year-to-year) and long-term climatic change (30-year periods or longer). This will be used to assess anthropogenic influence of hydroelectric regulation on freshwater exports. We develop a more robust regulation routine for the Hudson Bay HYPE (H-HYPE) model to simulate regulation of 15 NCRB reservoirs and to test the method on four reservoirs draining to the Arctic Ocean from Russia (Ob, Yenisey, and Lena rivers). Regulation rules are based on near-current operational storage-outflow relationships (2001–2010 for the NCRB, 1991 to 2000 for the Russian reservoirs) and do not account for new hydropower developments, altered power-sales markets, or system integration. This excludes dynamic or cascading reservoir optimization as has been demonstrated in other studies (Asadzadeh et al., 2014; Malekmohammadi et al., 2009; Cheng and Chau, 2004). We focus on rivers feeding the Nelson and Churchill Rivers; the two largest contributors of freshwater outflows to Southwestern Hudson Bay (Déry et al., 2011), both with increasing anthropogenic influence on their freshwater regimes since the 1970s (Déry et al., 2018) and four reservoirs throughout the Russian Arctic drainage basin. The methods presented aim to include monthly storage targets (as seen in Yassin et al., 2019) while also providing the option for more detailed and dynamic relationships between reservoir level and outflow.

### 1.1. Objective

The gap this work addresses is that of a reservoir regulation routine suitable for sub-basin discretized, continental-scale modelling that also considers daily target water surface levels. To bridge this gap, the objective of this work is to develop a reservoir regulation routine which can be applied to multiple reservoirs of significance in our study region simulated using the HYPE model by analyzing observations in a grammatical fashion. It must improve the modelling performance (short-term) and reliability (long-term) of simulated historical outflow in the most influential regulated reservoirs in the NCRB. This work also aims to reduce modelling reliance on prescribed outflow, as prescribed daily or monthly outflow schedules assume consistent interannual volume and timing of inflow (and climatic stationarity by extension). To achieve this objective, this work is broken into three main steps:

- 1) To develop a broadly applicable regulation routine synthesizing multiple types of processes used in industrial hydroelectric regulation models;
- 2) To develop an offline analysis tool to calibrate reservoir parameters before their inclusion in a continental-scale hydrologic model; and
- 3) To test multiple reservoir processes using historic storage-outflow relationships and select parameter sets which favour seasonal outflow and storage performance.

## 2. Study domains

This study focusses on simulating the regulation of 19 reservoirs from five river basins draining to the Arctic Ocean. Many of these reservoirs have a theoretical storage time of less than a year (no interannual storage; Fig. 1, Table 1). According to the modification of the natural river regime these basins are subject to “severe” (Nelson and Yenisey), “heavy” (Churchill and Ob), and “moderate” (Lena) regulation (by the river regulation index presented in Grill et al., 2015). In the NCRB, this regulated storage capacity is heavily leveraged to re-apportion the mixed-to-nival river regime (Stadnyk et al., 2019) to produce a hydrograph more consistent with hydroelectric production needs (i.e., inflows withheld in spring and summer, then released consistently throughout the winter; Déry et al., 2018). Reservoir physical characteristics and their basin climatic characteristics are presented in Tables 1 and 2, locations detailed in Fig. 1.

Reservoirs were selected where at least 15 months of overlapping reported Water Surface Level (WSL) and outflow data were available. These 15 months represent a relatively sparse eighth of the 10-year reference period used and sixteenth of the 20-year validation period. Daily discharge records (inflow and outflow) are obtained from the Water Survey of Canada (WSC, 2020) and the Global Runoff Data Centre (GRDC, 2020). Daily WSL records are obtained from the WSC (WSC, 2020) and reservoir levels at a 10-day repeat are obtained from the United States’ Department of Agriculture’s Foreign Agricultural Service Global Reservoirs and Lakes Monitor database (G-REALM; USDA-FAS, 2020). Reservoir surface areas and depths are obtained from the Global Lake and Wetland Database (GLWD; Lehner and Döll, 2004), the Global Lake Database v2 (Kourzeneva, 2010), and the Global Reservoir and Dam database v1.1 (GRAND: Lehner et al., 2016). Reservoir upstream area is reported from the Arctic-HYPE (A-HYPE, Andersson et al., 2015) hydrologic model. Live depth is the computed depth between the historic minimum and maximum WSLs since the onset of reservoir operations (post filling). Live storage is computed as the live depth multiplied by the reservoir surface area (HYPE reservoirs are modelled as rectangular prisms, accounting for no dynamic surface area). Detention time is the ratio of live storage to average inflow (over the period 1971 to 2015; Fig. 1, Table 2). Reservoirs simulated in this study have theoretical detention times between 0.2 and 24 months, examining the skill in

simulation of run-of-the-river reservoirs (little to no detention time) and large multi-year reservoirs (can theoretically store more than 12 months of inflow).

Mean annual upstream climatic conditions (total precipitation, snowfall, rainfall, temperature, potential evapotranspiration, and runoff) are computed from A-HYPE using the Hydrological Global Forcing Dataset for daily precipitation, daily max temperature, daily min temperature (HydroGFD; Berg et al., 2018). Abraham Lake in the Canadian Rocky Mountains and the Rafferty Reservoir in the Canadian Prairies represent the extremes in runoff ratio (equivalent runoff depth relative to total precipitation depth; 0.79 and 0.08, respectively; Table 2), aridity index (total precipitation relative to potential evapotranspiration; 2.38 and 0.52, respectively; Table 2), and snowfall ratio (snowfall relative to total precipitation; 0.57 and 0.19, respectively; Table 2). Remaining reservoirs span the gamut between these extremes representing various combinations of dryness, snowfall, and runoff efficiency. This gives a broad base of reservoir types (excluding rainforest or tropical conditions) on which to test a new reservoir regulation routine.

## 3. Methods and models

The skill of the HYPE model in simulating reservoir regulation has been tested for 19 reservoirs using two algorithms. The first is that belonging to HYPE in its current release, the second is that developed herein. The existing regulation algorithm in Arctic-HYPE version 3 (A-HYPE hereafter; Andersson et al., 2015) is described, as well as the development of the regulation used in Hudson Bay HYPE (H-HYPE hereafter; Stadnyk et al., 2020).

### 3.1. A-HYPE dam routine

The HYPE hydrological model (Lindström et al., 2010), developed by the Swedish Meteorological and Hydrological Institute (SMHI), discretizes watersheds to sub-basins, any of which can be (in part or in full) a lake or reservoir. Computation of the reservoir level and outflow is governed by a routine that simulates reservoir regulation. This HYPE dam routine includes sub-routines for four dam purposes: (1) flood control, (2) water supply, (3) irrigation, and (4) hydroelectric.

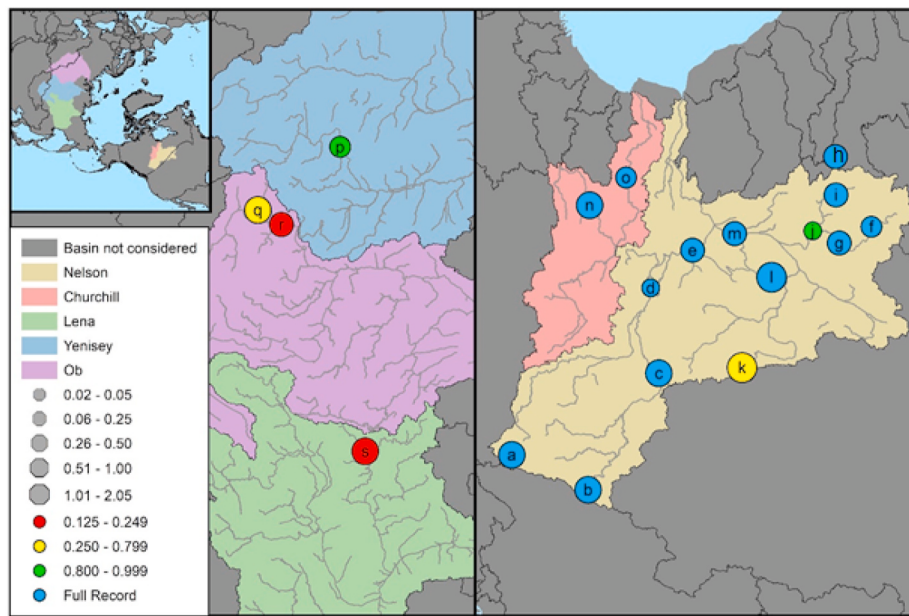


**Fig. 1.** Reservoir (size) theoretical maximum detention (live storage/mean inflow, expressed in years) and (colour) completeness of overlapping WSL and outflow records (as fraction of ten-year reference period). Labels correspond to all tables and figures. Labels correspond to all tables and Fig. 5 to 12.

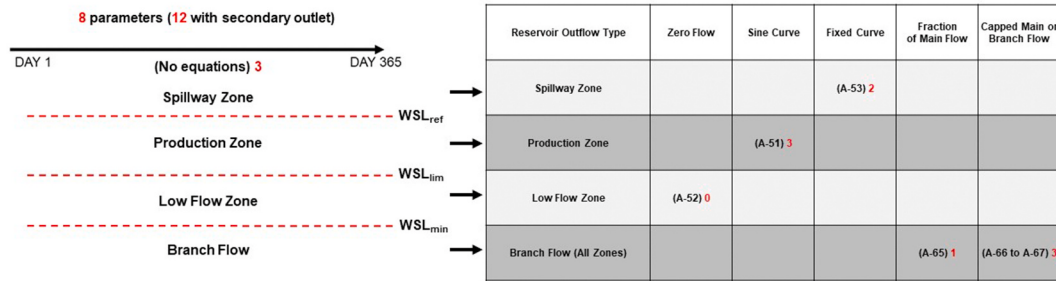


**Fig. 2.** Diagram describing A-HYPE dam regulation outflow equations used in each zone and total parameters used (red). Adapted from diagram found in SMHI's HYPE wiki ("Rivers and Lakes", 2020). Equations details available in Table A2 in Appendix A.

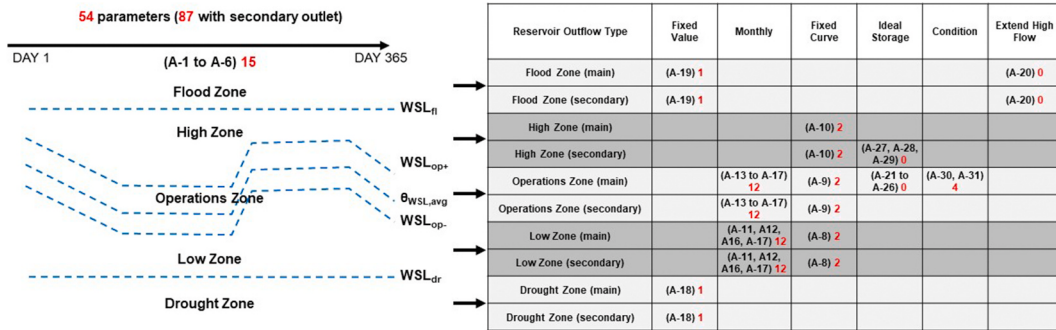


**Fig. 3.** Diagram describing H-HYPE regulation outflow equations used in each zone and total parameters used (red). Equations details available in Table A1 in Appendix A.

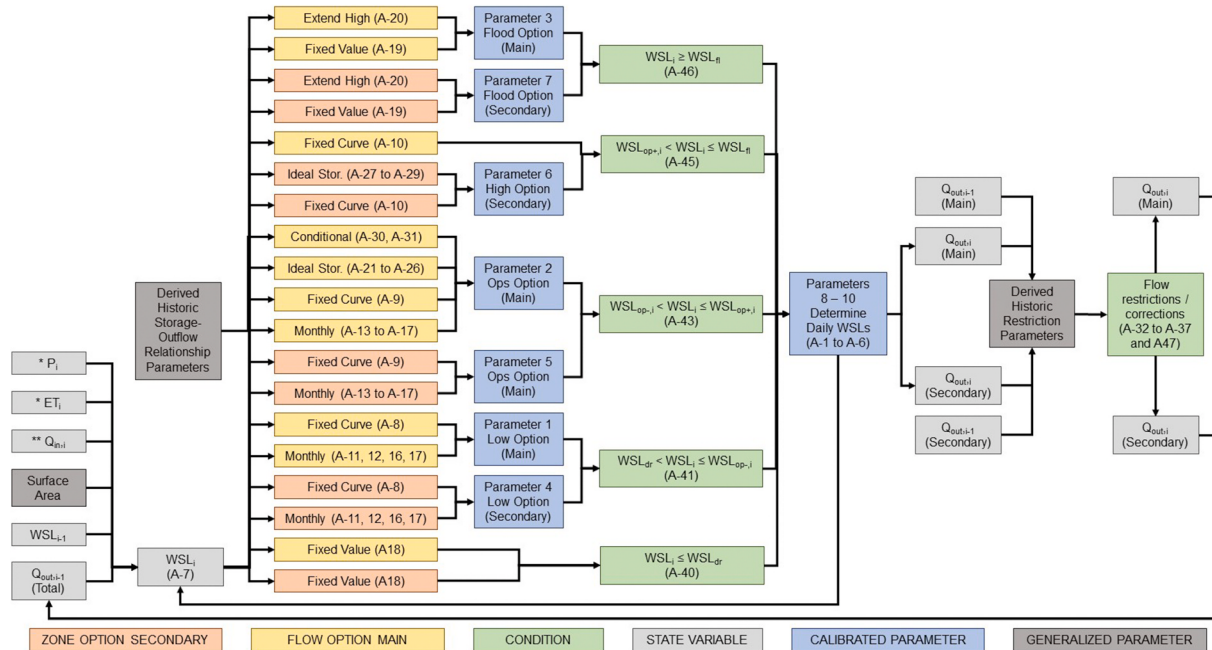


**Fig. 4.** Flowchart relating historic reservoir characteristics, parameters, and daily state variables, equations used appear in parentheses (as summarized in Appendix A). \* Computed in HYPE ("Processes above ground", 2020). \*\* Observed record used for this study.

Reservoirs can use one or two outlets (to simulate diversions). The existing HYPE routine for regulated dams focusses on physically based variables to produce a target daily outflow. Complete details regarding the routines governing dam outflow operations in HYPE can be found on SMHI's HYPE wiki under the Rivers and Lakes section ("River and Lakes", 2020).

Reservoirs in HYPE are modelled as rectangular storage units with

uniform surface area and variable level. Computation of outflow by time-step will access different elements of piecewise functions using the WSL computed for the previous time-step and two threshold parameters (called Minimum stage and Reference stages in Fig. 2). These stages divide the reservoir into three zones: low-flow zone (below Minimum stage), spillway-flow zone (above Reference stage), and production-flow zone (between Minimum and Reference stages). How much or little

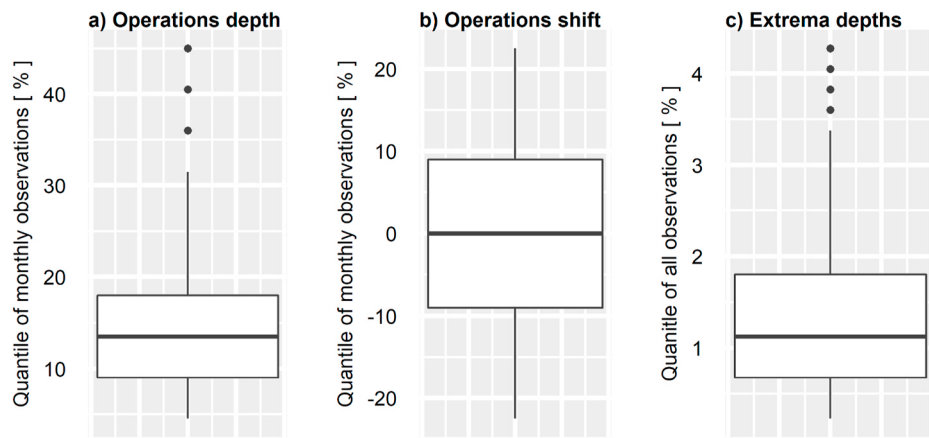


**Fig. 5.** Range of percentiles used to determine WSL stages ( $n = 610$ ). Boxplots describe interquartile range and median, whiskers extend to 1.5 times the interquartile range, dots for outliers.

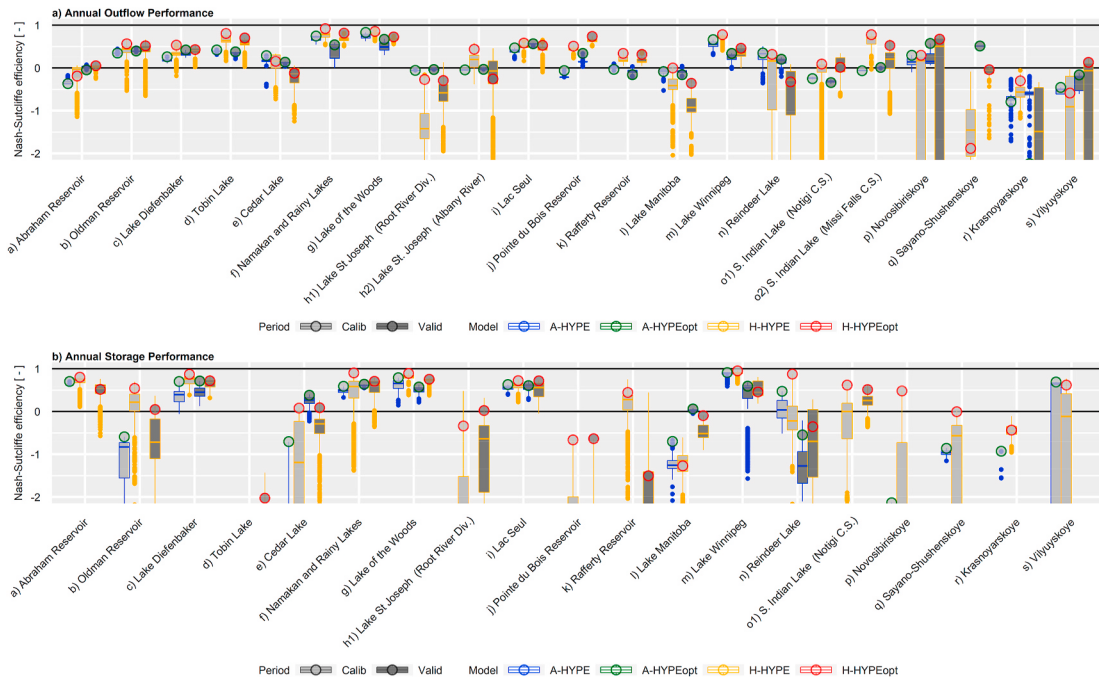


**Fig. 6.** Daily Nash-Sutcliffe efficiency (NSE) over full timeseries of (a) computed outflow and (b) computed storage in (light gray) reference and (dark gray) validation periods. Presented as a boxplot for all simulated instances of (blue) A-HYPE and (orange) H-HYPE, with selected optimum presented as a point for (green) A-HYPE and (red) H-HYPE. Boxplots describe interquartile range and median, whiskers extend to 1.5 times the interquartile range, dots for outliers. Labels correspond to all tables and figures. Labels correspond to all tables and Fig. 1 and 6 to 13. Note that validation period data do not exist for Russian reservoirs (p, q, r, and s).

water is discharged daily from the reservoir in the production-flow zone will depend on the dam's purpose, specified by the user. All reservoirs compared in this work were calibrated using the existing HYPE regulation routine (Stadnyk et al., 2019, 2020) as hydroelectric dams with a sine curve outflow when in the production zone (Fig. 2; Equation A-51, Table A2, Appendix A), a weir-type equation in the spillway zone (Fig. 2; Equation A-53, Table A2, Appendix A). These relationships result in seven parameters for single outlet reservoirs: two WSL thresholds, three sine-function parameters (amplitude, phase, mean), and two parameters for the spillway (coefficient and exponent of a power curve). Four additional parameters are added for bifurcated (branched) reservoirs: minimum and maximum main outlet flow, maximum branch flow, and the desired fraction of total flow to the branched outlet ("Rivers and Lakes", 2020). Methods exist in A-HYPE to specify two means of the sine-function split by two datums (expressed in days). These methods

are not employed here as the means to split historical records intra-annually by varying dates are not considered.

### 3.2. H-HYPE dam routine development

A new reservoir regulation routine is presented for the HYPE model (tested in R, to be written into HYPE in Fortran). Access to the HYPE code was provided by SMHI for the purposes of this project. This new routine ties together operations and modelled state variables, maintaining applicability to reservoirs of many types of operation and many sizes. This applicability allows the routine to be applied to any reservoir which modellers wish to represent with a minimum of operational knowledge necessary prior to running the model.

The new routine formulation is the synthesis of the processes of nine reservoir regulation models developed by Manitoba Hydro, each

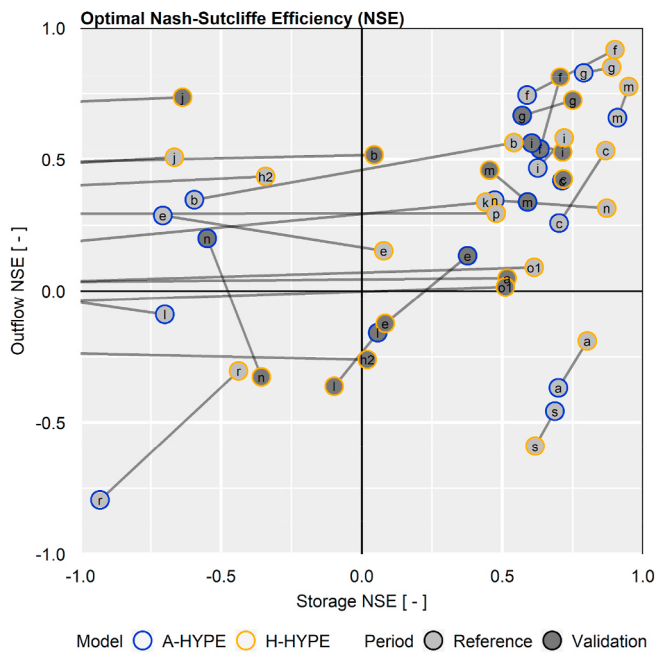


**Fig. 7.** Optimal selection Nash Sutcliffe Efficiency [-] for all reservoirs in (dark gray) validation and (light gray) reference periods for (blue) A-HYPE and (orange) H-HYPE presented as scatter of storage and outflow. Gray lines tie individual A-HYPE and H-HYPE performances. Labels correspond to all tables and Fig. 1 and 6 to 13.

governing a single reservoir. As in A-HYPE, each of these models uses a fixed set of stage-wise processes (i.e., monthly storage-outflow curves, minimum ecological outflow, target outflow by day-of-year, etc.) for a

varying number of reservoir thresholds (fixed stages or stage curves). A model is developed with multiple possible formulations (Fig. 3) of the piecewise function governing outflow, with parameters derived from historical stage-outflow relationships.

The reservoir is divided into five zones based on two fixed stages and two stage curves. The zone and level of the reservoir for each simulated time-step will dictate outflow equation used and overall volume of outflow. For timestep  $i$ , month  $j$ , general versions of the formulation are presented. Stages, zones, and options for each zone are summarized in Fig. 3. ‘‘Fixed Value’’ (Equations A-18 and A-19, Table A1, Appendix A) indicates that when the simulated WSL is in that zone, the outflow is a fixed value (allowable maximum or minimum). ‘‘Monthly’’ (Equation (1) below; Equations A-11 to A-17, Table A1, Appendix A) indicates a monthly, linear storage-outflow relationship for WSLs within that zone for that month (above  $WSL_{\beta_j}$ , which varies monthly). ‘‘Fixed Curve’’ (Equation (2) below; Equations A-8 to A-10, Table A1, Appendix A) indicates an exponential storage-outflow relationship within that zone (above  $WSL_a$ ). ‘‘Ideal Storage’’ (Equation (3) below; Equations A-21 to A-29, Table A1, Appendix A) methods use the distance between the current day’s WSL and the target storage curve ( $\theta$ , not a parameter) as well the previous two weeks’ inflow and previous two weeks gradient of the target storage curve to dictate outflow. ‘‘Condition’’ (Equation (4) below; Equations A-30 and A-31, Table A1, Appendix A) indicates a relationship between the outflow of the reservoir and an external timeseries (outflow of another sub-basin). Fifteen parameters govern the threshold stages of WSL: 12 parameters for target storage on the first day of each month, the depth of the operations zone, the flood stage, and the drought stage. Fixed values introduce two parameters (flood maximum and drought minimum outflow) per outlet, monthly relationships: 24 (one coefficient  $\alpha_j$  per month, two zones) per outlet, fixed curves: six (one coefficient  $\gamma$  and power  $\varepsilon$ , three zones) per outlet, with an additional parameter for maximum daily change of outflow, conditional flow introduces four parameters ( $\mu$ ,  $\rho$ ,  $\tau$ , and  $\omega$ ).

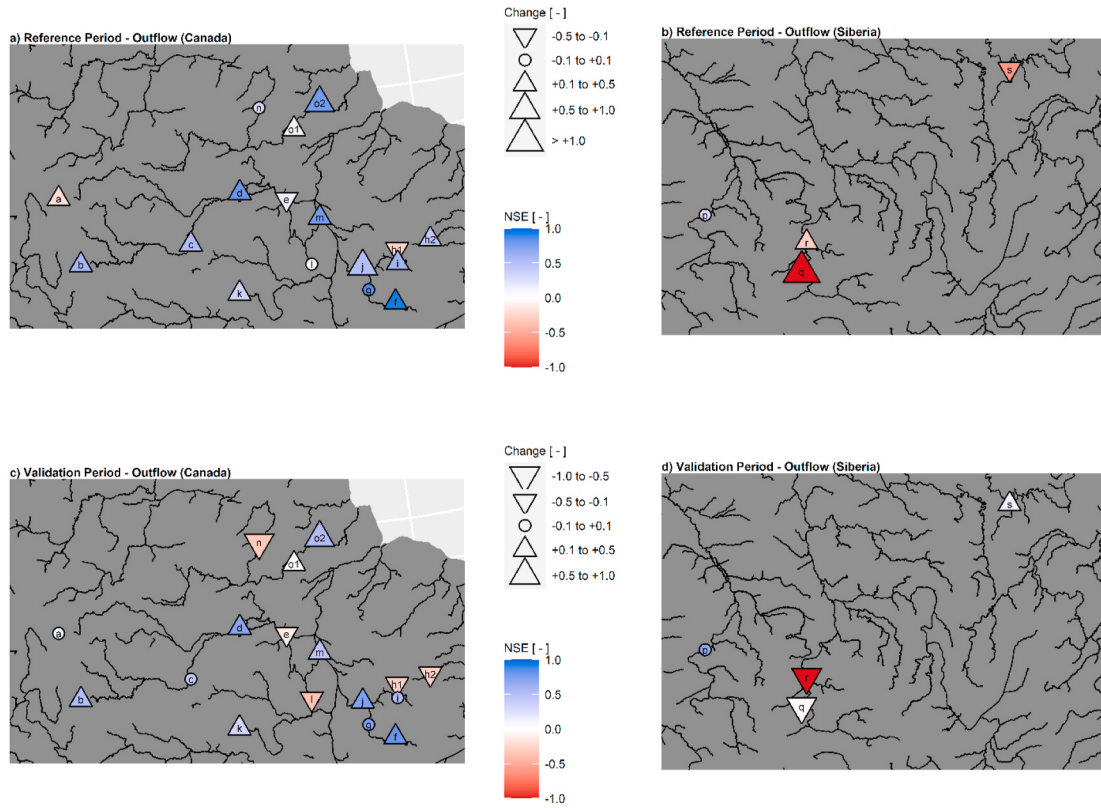


**Fig. 8.** Mapped daily Nash-Sutcliffe efficiency (NSE) of computed outflow for (a, b) reference period and (c, d) validation period in (a, c) Canadian and (b, d) Russian reservoirs. Colour indicates H-HYPE selected optimum, shape and size indicate change relative A-HYPE. Labels correspond to all tables and Fig. 1 and 6 to 13.

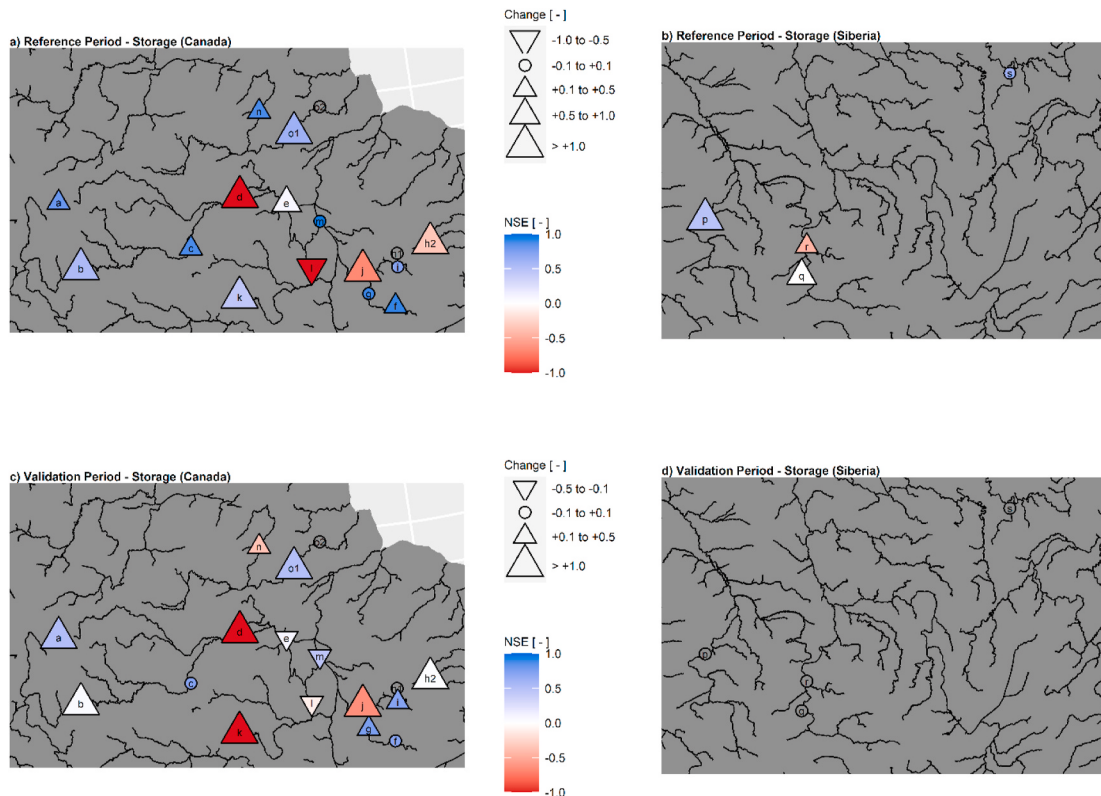


**Fig. 9.** Mapped daily Nash-Sutcliffe efficiency (NSE) of computed storage for (a, b) reference period and (c, d) validation period in (a, c) Canadian and (b, d) Russian reservoirs. Colour indicates H-HYPE selected optimum, shape and size indicate change relative A-HYPE. Labels correspond to all tables and Fig. 1 and 6 to 13.

$$Q_i = \alpha_j \times (WSL_i - WSL_{\beta, j})$$

$$Q_i = \gamma \times (WSL_i - WSL_\delta)^e$$

$$Q_i = (\theta + 1) \times \left( \frac{\sum_{i=13}^i Q_{in, i}}{14} \right) + \frac{\sum_{i=13}^i (S_i - S_{i+1})}{14}$$

$$Q_i = \mu \times (Q_{external} - \rho)^r - \omega$$

The applicability of this routine is tested by deriving parameters (stage-outflow relationships derived based on paired observed data from a reference period, not calibrated) and simulating outflow and storage over 30 years. The use of this new regulation routine is meant as a proof of concept to demonstrate that a diverse set of reservoirs can be simulated using paired, observed data without prior knowledge of reservoir operations.

The routine presented does not pre-suppose a prior understanding of what processes govern outflow computation within different zones of the reservoir (excluding drought zone) for any given reservoir and uses an offline tool (R function external to the HYPE model) to test combinations of processes and select the optimal set of processes. By testing multiple combinations of piecewise flow processes (referred to as zone-options; Figs. 3 and 4; Table 3), we avoid applying empirical regulation codes based on real-world operations specific to individual reservoirs. This aims to avoid the “black-box” effect (Kirchner, 2006) if coded directly into a hydrologic model.

This routine aims to reduce parametric uncertainty (an issue highlighted by Beven, 2012; Juston et al., 2013) by making use of physically-based processes rather, unlike operation schemes using neural networks or hidden logic, which have also been applied successfully in macro-scale modelling schemes (Coerver et al., 2018; Ehsani et al., 2016). An important element of this routine is the interannually variable storage rule curves (which govern the low, operations, and high zone in

(1) H-HYPE; Fig. 3) rather than fixed thresholds for piecewise operations throughout the year (three zones in A-HYPE; Fig. 2). Use of variable target storage values throughout the year are shown to improve reservoir model performance (Yassin et al., 2019; Wu and Chen, 2012) by imposing seasonally or monthly variant thresholds to reservoir outflow behaviour.

For each reservoir, a statistically optimal set of options (process dictating outflow for each zone) is generated by the Reservoir Analysis Tool (RAT; Section 3.3; reported in Table 3). A description of the function of the regulation routine within each timestep is shown in Fig. 4. It further helps describe the use of the daily outflow to calculate storage (calculated from the WSL) for the next timestep. Section 3.4 describes the process used to systematically mix the integer parameters and WSL limits for both models. Section 4 describes the results of these multiple simulations.

Optimal storage-outflow relationships (whether linear monthly or fixed curve) are derived using the RAT and near-current WSL and outflow records (2001–2010 for Canadian reservoirs, 1991 to 2000 for Russian reservoirs), referred to as the reference period. This reference period is selected to provide the most up-to-date possible regulation rules for the studied historical period. Though these equations introduce parameters to the formulation the parameters are designed to be kept fixed relative to a set of governing stages. In this way, because the parameters are related to historical physical observations, they are similar to other fixed variables, such as reservoir surface area, in that they are untouched by optimization. Using fixed parameters based on historical storage-outflow relationships is proven to provide adequate, though not optimal, modelling of reservoirs performance compared to simpler methods (referred to as a “generalized parameter set” by Yassin et al., 2019), while offering the option to improve performance with a full optimization, with 610 sets of WSLs tested here to vary the stage-discharge relationships.

The A-HYPE parameters defining the minimum stage and spillway

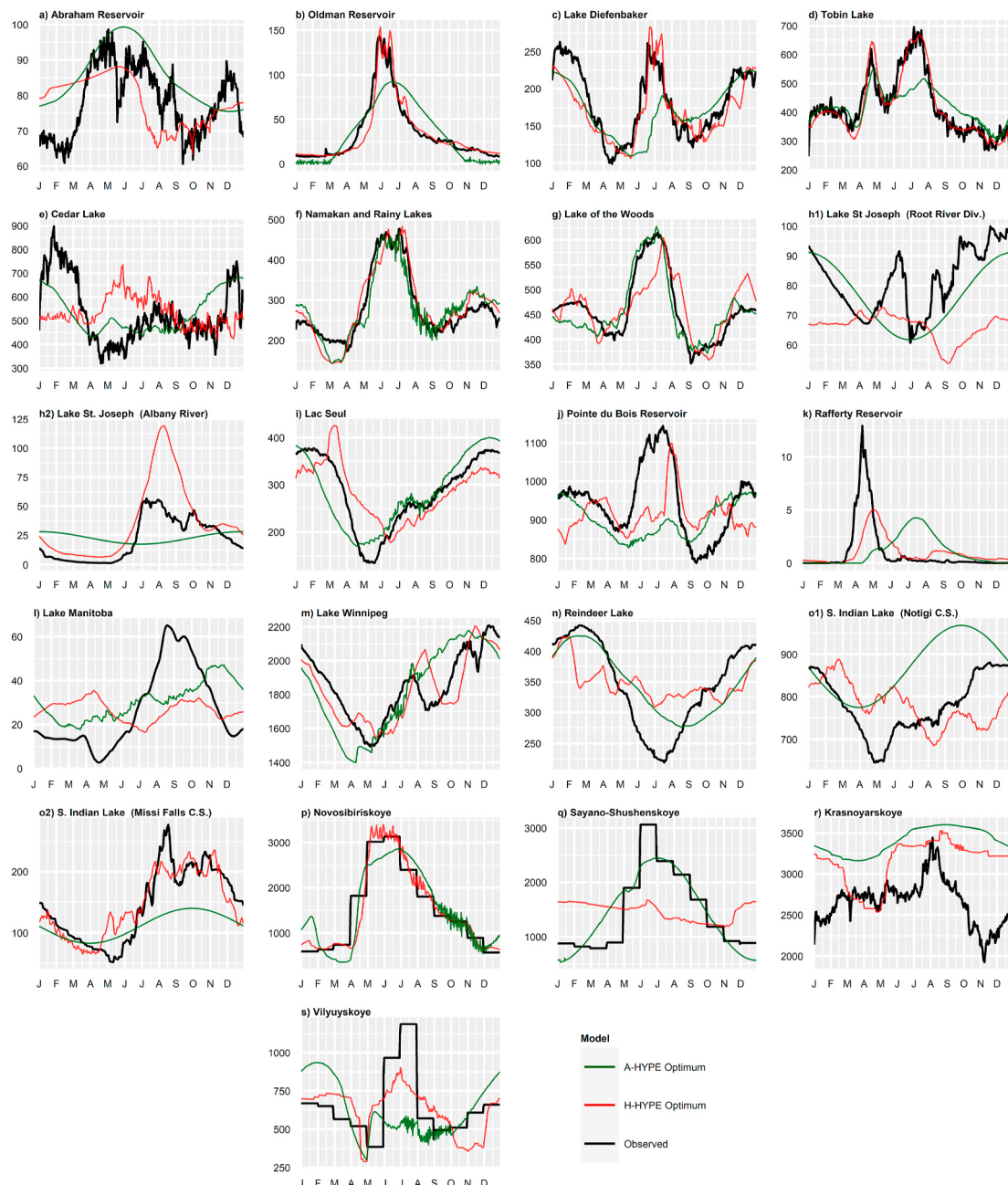


**Fig. 10.** Average annual daily outflow (all in cubic metres per second) for (black) observed, (green) optimal A-HYPE parameters, and (red) optimal H-HYPE parameters. Labels correspond to all tables and Fig. 1 and 6 to 13.

stage are defined as the minimum and maximum limits of the derived H-HYPE operations stage curves ( $WSL_{op}$ - and  $WSL_{op+}$ , respectively; Fig. 3). Parameters defining the storage-outflow relationship of the spillway curve (Equation A-28, Table A1, Appendix A) are derived using LSR on all paired data above the spillway stage ( $WSL_{reference}$ ; Fig. 2), log-transformed to linearize the data. Parameters defining the sine curve are computed using observed outflow where WSL falls in the defined operations zone (Fig. 2). Errors are minimized between a synthetic sine curve (using amplitude, mean and phase) and that defined by the reference period production zone average annual daily (Equation A-27, Table A; Appendix A).

### 3.3. Reservoir analysis tool (RAT)

Before introducing new reservoirs to H-HYPE, reservoir process

selection (narrowing the zone-options of Fig. 3 to a single set, as shown in Fig. 4, details in Table 3) is automated using the RAT. This tool replicates the routine added to H-HYPE, without the need to run an entire HYPE simulation. To directly compare the skill of the reservoir regulation, rather than the full hydrologic model, reservoirs were compared by supplying each reservoir with its observed daily inflow timeseries. Precipitation onto reservoirs is taken from the HydroGFD dataset and reservoir evaporation losses are calculated in A-HYPE using the Priestley-Taylor method, where the difference between maximum and minimum daily air temperature approximates radiative forcing ("Processes above ground", 2020) and assuming that lakes act as free evaporation surfaces. Each reservoir is simulated as a sub-basin in A-HYPE and H-HYPE eliminating the need for a volume and/or momentum-based methods to pass water within a reservoir between grid-cells or sub-basins, as seen in Shin et al. (2019).

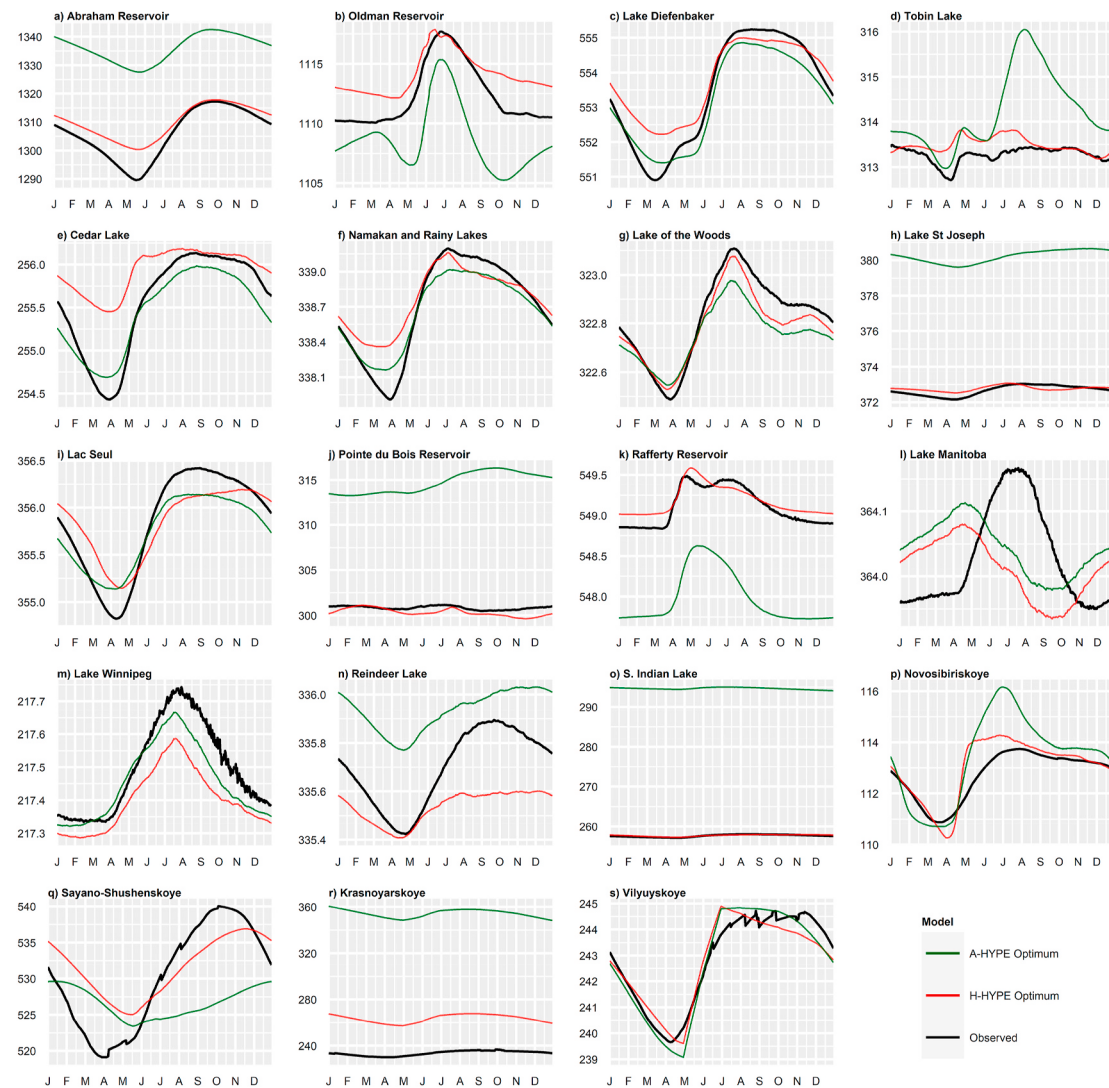


**Fig. 11.** Average annual daily water surface level (all in metres above surface level) for (black) observed, (green) optimal A-HYPE parameters, and (red) optimal H-HYPE parameters. Labels correspond to all tables and Fig. 1 and 6 to 13.

Functioning of the RAT offline from HYPE relies on complete inflow records. These are developed for each reservoir using public records from the WSC, GRDC, or using synthetic methods. Shorter gaps in observed inflow records ( $\leq 2$  days) were filled using linear interpolation. Where significant gaps exist in inflow records ( $> 2$  days), gap-filling was performed using the next upstream gauge (available from the [WSC, 2020](#) or [GRDC, 2020](#)) and proportional drainage area scaling ([Déry et al., 2005, 2011](#); [Hernández-Henríquez et al., 2010](#)). Outflow, and WSL are not gap-filled since these data are used exclusively to evaluate performance and develop storage-outflow relationships. These records can be found in [Table A3, Appendix A](#).

Where no inflow data are available, synthetic time series of inflow are generated. These are created using the relationship between throughflow and storage (Equations (5) and (6) where  $SA$ : reservoir surface area [ $m^2$ ],  $Q_{in}$ : daily inflow [ $m^3 \text{ day}^{-1}$ ],  $Q_{out}$ : daily outflow [ $m^3 \text{ day}^{-1}$ ],  $WSL$ : daily water surface level [m],  $\Delta S$  is daily storage change [ $m^3$ ],  $P$ : daily precipitation [mm],  $ET$ : daily total evapotranspiration [mm], between days  $i$  and  $i-1$  or  $\Delta t$ : timestep [day]). Records were further synthetically extended by using the average annual daily value of existing data. These existing gaps are ignored during statistical calculations so as not to introduce added uncertainty into parameter estimation. Uses of full records and synthetic inflow series are summarized in [Table A3, Appendix A](#). [Table A1 \(Appendix A\)](#) presents the input

records used for parameter derivation (outflow and WSL) and simulation (inflow, precipitation, and evaporation).

$$SA(WSL_i - WSL_{i-1}) = \Delta S = \Delta t \left( Q_{in, i} - Q_{out, i-1} + SA \frac{(P - ET)}{10^3} \right) \quad (5)$$

$$Q_{in, i} = SA \left( \frac{(WSL_i - WSL_{i-1})}{\Delta t} + \frac{ET - P}{10^3} \right) + Q_{out, i-1} \quad (6)$$

The scope of the BaySys group of projects excludes optimization of cascading reservoirs. Reservoirs are calibrated individually on their individual skill scores, not on an aggregated basin-wide score. Regulation rules are also designed to be static. These rules do not change or adapt to future climatological conditions. To achieve reliable results with these static rules, the reservoir operation routines must strive to maintain desirable reservoir levels, rather than dictating optimal outflow values as inflow volume and timing are likely to change in the future. Dynamic optimization of reservoirs for power production or financial gain is ignored, with the maintenance of reservoir levels consistent with historic operations prioritized instead.

### 3.4. Optimal selection

The RAT simulates 610 sets of stage limits by modifying operations

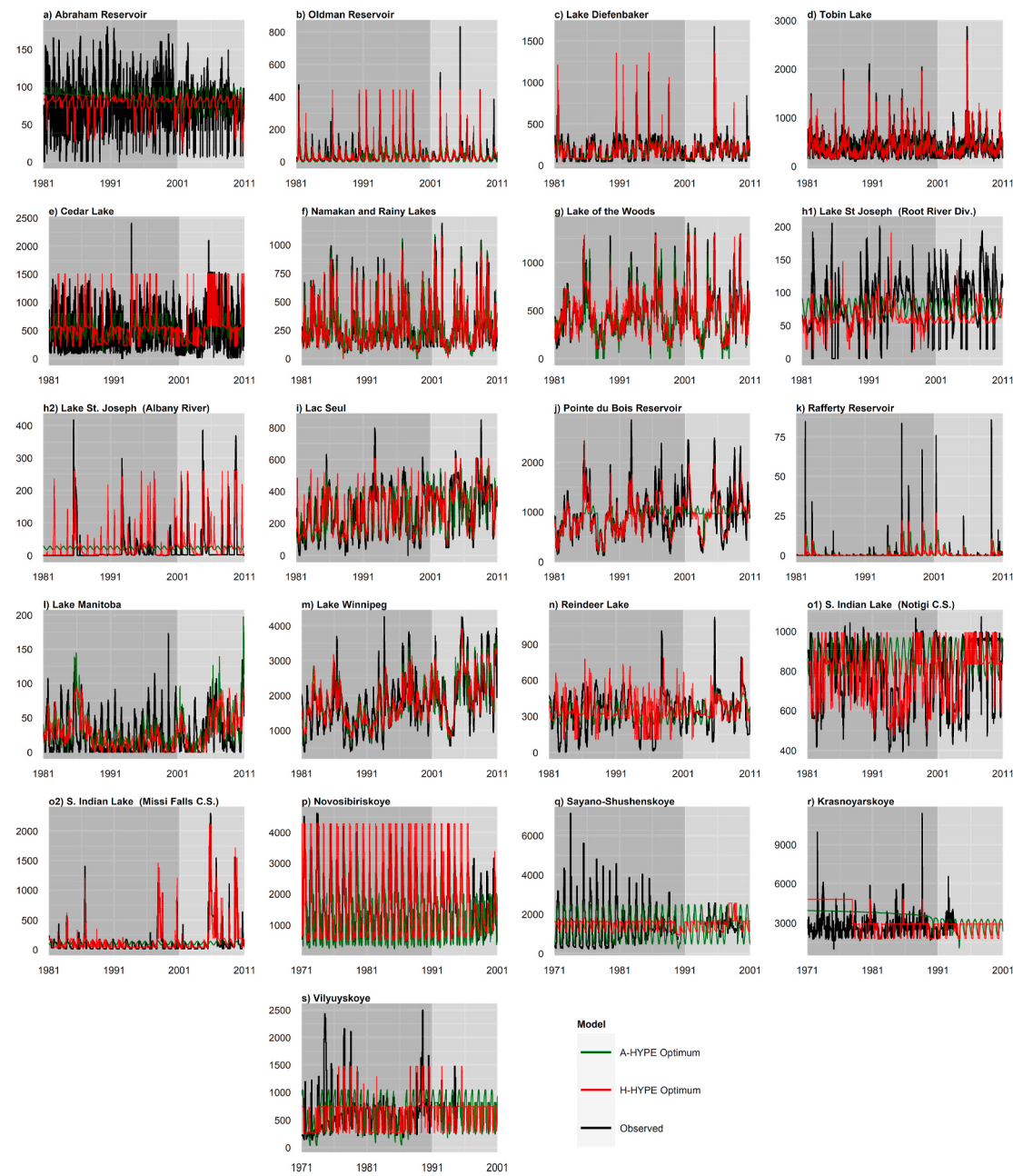


**Fig. 12.** Daily outflow (all in cubic metres per second) for (black) observed, (green) optimal A-HYPE parameters, and (red) optimal H-HYPE parameters. Shaded areas for (dark gray) validation period and (light gray) reference period. Labels correspond to all tables and Fig. 1 and 6 to 13.

depth, operations shift, and extreme stage depth in H-HYPE (described in Section 3.2, ranges presented in Fig. 5), which relate to  $WSL_{\text{minimum}}$  and  $WSL_{\text{reference}}$  (A-HYPE), evaluating all H-HYPE zone-option combinations (16 for a single-outlet or 256 for a double-outlet reservoir) and the associated A-HYPE options (1 for a single outlet or 2 for a double outlet reservoir) for each set of stage limits. Outflow and storage performance (of  $610 \times 16 = 9760$  or  $610 \times 256 = 156160$  timeseries for H-HYPE, 610 or 1220 timeseries for A-HYPE) is used to select an optimal parameterization for each model. This selection is based on the performance of daily timeseries in the reference period (1 January 2001 to 31 December 2010 for Canadian and 1 January 1991 to 31 December 2000 for Russian reservoirs). These periods are split into seasonal timeseries using standard hydrological seasons (winter: DJF, spring: MAM, summer: JJA, autumn: SON). This performance is then validated for an earlier period (1 January 1981 to 31 December 2000 for Canadian and 1 January 1971 to 31 December 1990 for Russian reservoirs). Reference

periods are selected to maximize overlapping WSL and outflow records, with validation periods taken as the preceding twenty years.

The combined (outflow and storage) performance is computed to select the optimal stage limits and zone-options. This is taken as the sum of seasonal outflow and storage Nash-Sutcliffe Efficiencies (NSE, [Nash and Sutcliffe, 1970](#)) of daily timeseries ( $4 \text{ seasons} \times 2 \text{ variables} = 8$ ). Where there were two outlets, the sum of NSEs for all seasons for storage and outlets is optimized ( $4 \text{ seasons} \times 3 \text{ variables} = 12$ ). Seasonal NSE is used rather than the seasonal Kling-Gupta Efficiencies (KGE; [Gupta et al., 2009](#)) due to the NSE being shown to be more sensitive in calibration of reservoir regulation in H-HYPE ([Stadnyk et al., 2020](#)). The ideal combination of zone-options and stages (Table 3) is selected as the greatest sum of NSEs.

The number of equifinal solutions are listed in Table 3 as a fraction of the total number of combinations assessed. Equifinality is seen in A-HYPE in both reservoirs with two outlets (Lake St. Joseph and Southern

**Table 1**

Reservoir physical characteristics and operations details. Live depth computed from historic operational records, surface area from GLWD, commissioning date stated as the start of operation (excluding construction or filling).

Label	Reservoir	Control Structure(s)	Current Operator(s)	Commission Year	River	Basin	Live Depth [m]	Surface Area [km <sup>2</sup> ]
a	Abraham Reservoir	Bighorn Dam GS	TransAlta	1972	North Saskatchewan River	Nelson	29.7	69
b	Oldman Reservoir	Oldman River CS	ATCO	1991	Oldman River	Nelson	30.0	22
c	Lake Diefenbaker	Gardiner Dam CS/Coteau Creek GS	SWSA/ SaskPower	1967	South Saskatchewan River	Nelson	7.2	458
d	Tobin Lake	E. B. Campbell GS	SaskPower	1963	Saskatchewan River	Nelson	1.0	262
e	Cedar Lake	Grand Rapids GS	Manitoba Hydro	1962	Saskatchewan River	Nelson	2.9	2817
f	Namakan Lake/Rainy Lake	Fort Frances GS/Kettle Falls GS	IJC/RLWWB	1914	Rainy River	Nelson	1.7	1274
g	Lake of the Woods	Whitedog GS/Norman GS	IJC/LWCB	1912	Winnipeg River	Nelson	1.3	4168
h	Lake St Joseph	Root Portage Diversion CS	IJC/OPG	1958	Root River/Albany River	Nelson/ Albany	2.2	628
i	Lac Seul	Ear Falls GS	IJC/OPG	1928	English River	Nelson	2.6	1611
j	Pointe du Bois Reservoir	Pointe du Bois GS	Manitoba Hydro	1958	English River	Nelson	3.7	287
k	Rafferty Reservoir	Rafferty Dam CS	SWSA	1994	Souris River	Nelson	2.7	33
l	Lake Manitoba	Fairford River CS	MIT	1961	Fairford River	Nelson	0.6	4790
m	Lake Winnipeg	Jenpeg GS	Manitoba Hydro	1979	Nelson River	Nelson	1.4	23809
n	Reindeer Lake	Whitesand Dam CS	SaskPower	1942	Reindeer River	Churchill	1.8	5596
o	Southern Indian Lake	Missi Falls CS/Notigi CS	Manitoba Hydro	1977	Churchill River/Rat River	Churchill/ Nelson	1.3	2227
p	Novosibirskoye	Novosibirsk GS	RusHydro	1950	Ob River	Ob	3.2	954
q	Sayano-Shushenskoye	Sayano-Shushenskaya GS	RusHydro	1985	Yenisey River	Yenisey	23.3	1228
r	Krasnoyarskoye	Krasnoyarsk GS	RUSAL	1972	Yenisey River	Yenisey	12.0	1884
s	Vilyuyanskoye	Vilyuy Dam GS	Alrosa	1973	Vilyuy River	Lena	7.5	2077

GS: Generating Station; CS: Control Structure; Alberta Trailer Company (ATCO), Saskatchewan Water Security Agency (SWSA), International Joint Commission (IJC); Rainy-Lake of the Woods Watershed Board (RLWWB), Lake of the Woods Control Board (LWCB); Ontario Power Generation (OPG); Manitoba Infrastructure and Transportation (MIT); Russian Aluminium (RUSAL).

**Table 2**

Reservoir and upstream climatic characteristics. Average total annual precipitation (P) directly from HydroGFD (Berg et al., 2018). Annual total potential evapotranspiration (PET), snowfall (S), and runoff (R) simulated from Arctic-HYPE (Andersson et al., 2015) using HydroGFD as input. Mean inflow computed from WSC (WSC, 2020) or GRDC (GRDC, 2020) records. Upstream area from Arctic-HYPE delineations. Inflow, R, S, P, and PET computed from daily data over the period 1971 to 2015. Detention time computed as ratio of live storage to mean inflow.

Label	Reservoir	Upstream Area [km <sup>2</sup> ]	Detention Time [months]	Mean Inflow [m <sup>3</sup> s <sup>-1</sup> ]	Aridity Index (P/PET) [-]	Runoff Ratio (R/P) [-]	Snowfall Ratio (S/P) [-]
a	Abraham Reservoir	3921	9.8	79.31	2.382	0.793	0.566
b	Oldman Reservoir	4135	7.0	35.72	1.381	0.584	0.423
c	Lake Diefenbaker	155162	6.2	200.2	0.658	0.246	0.300
d	Tobin Lake	343315	0.2	450.2	0.703	0.248	0.287
e	Cedar Lake	394024	5.3	576.2	0.731	0.267	0.283
f	Namakan Lake/Rainy Lake	37222	2.9	280.9	1.588	0.576	0.210
g	Lake of the Woods	69457	4.5	445.8	1.464	0.542	0.197
h	Lake St Joseph	14011	5.3	99.28	1.666	0.605	0.277
i	Lac Seul	26210	5.7	277.7	1.604	0.584	0.259
j	Pointe du Bois Reservoir	122898	0.4	958.4	1.498	0.553	0.219
k	Rafferty Reservoir	10258	13.9	2.469	0.521	0.078	0.189
l	Lake Manitoba	86179	24.2	41.37	0.886	0.355	0.241
m	Lake Winnipeg	1006783	5.9	2195	0.832	0.326	0.237
n	Reindeer Lake	65001	11.3	330.9	1.250	0.561	0.313
o	Southern Indian Lake	264705	1.2	983.1	1.164	0.490	0.278
p	Novosibirskoye	226090	0.8	1517	1.154	0.479	0.287
q	Sayano-Shushenskoye	185703	7.3	1488	1.270	0.549	0.263
r	Krasnoyarskoye	294933	3.2	2655	1.327	0.548	0.262
s	Vilyuyanskoye	134082	9.2	646.7	1.125	0.576	0.384

Indian Lake, “h” and “o” in Figs. 6 to 12) and two others (Abraham and Rafferty Reservoirs) and two reservoirs in H-HYPE (two matching optima in each case). In both models, these values represent a negligible fraction of the total range of WSLs (A-HYPE and H-HYPE) or integer options (H-HYPE) tested.

#### 4. Results and discussion

Fig. 6 presents the A-HYPE and H-HYPE values of NSE for continuous, daily timeseries (n = 3652 for reference and n = 7304 for validation periods). The sums of seasonal statistics (maximum sum of NSEs) are used to inform the selection of processes in the RAT. The selected, best performing RAT parameter set is shown for each outlet as well as its A-HYPE counterpart, with the optimal performance for two performance

**Table 3**

Optimal H-HYPE zone-options selected. Names of options correspond to Figs. 3 and 4 and labels correspond to all tables and Figs. 1 and 6 to 13. Number of equifinal results are computed relative to optimal simulation.

Label	Reservoir	Drought Option	Low Option	Operations Option	High Option	Flood Option	Equifinal Results/Total Results	
							A-HYPE	H-HYPE
a	Abraham Reservoir	Fixed Value	Monthly	Fixed Curve	Fixed Curve	Extend High	2/610	0/7320
b	Oldman Reservoir	Fixed Value	Monthly	Ideal Storage	Fixed Curve	Fixed Value	0/610	0/7320
c	Lake Diefenbaker	Fixed Value	Fixed Curve	Ideal Storage	Fixed Curve	Fixed Value	0/610	0/7320
d	Tobin Lake	Fixed Value	Fixed Curve	Fixed Curve	Fixed Curve	Extend High	0/610	1/7320
e	Cedar Lake	Fixed Value	Fixed Curve	Monthly	Fixed Curve	Fixed Value	0/610	0/7320
f	Namakan Lake/Rainy Lake	Fixed Value	Monthly	Ideal Storage	Fixed Curve	Extend High	0/610	0/7320
g	Lake of the Woods	Fixed Value	Monthly	Monthly	Fixed Curve	Fixed Value	1/610	0/7320
h1	Lake St Joseph	Fixed Value	Fixed Curve	Ideal Storage	Fixed Curve	Fixed Value	1/1220	0/155160
h2		Fixed Value	Monthly	Monthly	Fixed Curve	Fixed Value		
i	Lac Seul	Fixed Value	Monthly	Fixed Curve	Fixed Curve	Fixed Value	0/610	0/7320
j	Pointe du Bois Reservoir	Fixed Value	Monthly	Ideal Storage	Fixed Curve	Fixed Value	0/610	0/7320
k	Rafferty Reservoir	Fixed Value	Monthly	Ideal Storage	Fixed Curve	Extend High	4/610	0/7320
l	Lake Manitoba	Fixed Value	Monthly	Monthly	Fixed Curve	Fixed Value	0/610	1/7320
m	Lake Winnipeg	Fixed Value	Monthly	Monthly	Fixed Curve	Fixed Value	0/610	0/7320
n	Reindeer Lake	Fixed Value	Fixed Curve	Ideal Storage	Fixed Curve	Fixed Value	0/610	0/7320
o1	Southern Indian Lake	Fixed Value	Monthly	Ideal Storage	Fixed Curve	Fixed Value	1/1220	0/155160
o2		Fixed Value	Fixed Curve	Monthly	Fixed Curve	Fixed Value		
p	Novosibirskoye	Fixed Value	Monthly	Ideal Storage	Fixed Curve	Fixed Value	0/610	0/7320
q	Sayano-Shushenskoye	Fixed Value	Monthly	Ideal Storage	Fixed Curve	Fixed Value	0/610	0/7320
r	Krasnoyarskoye	Fixed Value	Monthly	Ideal Storage	Fixed Curve	Fixed Value	1/610	0/7320
s	Vilyuyuskoye	Fixed Value	Monthly	Ideal Storage	Fixed Curve	Fixed Value	0/610	0/7320

metrics (NSE and percent error of standard deviation) presented for both models, reference and validation periods, outflow and storage in Tables 4 and 5 and mapped spatially in Figs. 8 and 9.

Testing 610 sets of base WSL characteristics (Fig. 5) and evaluating all possible simulations with related parameters gives a range of results for both models. Examining boxplot performance, the bottoms of the interquartile ranges (Fig. 6) of the full timeseries H-HYPE are in some cases higher than the top of A-HYPE for the same. This is the case for the full timeseries (“Annual”) storage in 10 (reference) and 7 (validation) of 19 reservoirs and outflow in 13 (reference) and 8 (validation) of 21 outlets (Fig. 6). This demonstrates that not only is the optimal solution improved (Figs. 7–9; Tables 4, 5), there is increased probability of stronger performance even if the selection of an optimum may contain uncertainty, such as that due to the choice of selection metric. Seasonal improvements can be seen in the daily optimal simulation (Figs. 12 and

13) as well as in the mean regime (average annual daily; Figs. 10 and 11) over the 30 years of the reference and validation combined periods.

Fig. 7 presents the optimal results selected for each reservoir (also seen in Fig. 6). In nine and eight of 21 outlets (for validation and reference, respectively; Fig. 7), the NSE of outflow simulated in H-HYPE is greater than 0.5, considered the threshold for “satisfactory” performance for watershed scale hydrological simulation by Moriasi et al., (2015) compared to three and five for the same in A-HYPE. While these results are initially overwhelming, we must remember that these simulations are governed by historical relationships (i.e., storage-outflow relationships), compared against measured data which are governed by human judgement, highly interconnected operational systems, and individual dam operators. This does not excuse poor NSE performance but should be considered when contextualizing the difficulty in simulating short scale human operations rather than the

**Table 4**

Respective optimal NSE for A-HYPE and H-HYPE models for outflow and storage over reference (2001–2010 for Canada, 1991 to 2000 for Russia) and validation (1981–2000 for Canada, 1971 to 1990 for Russia) periods. Validation storage listed as “N/A” for Russian reservoirs due to lack of observed data. Values less than –3.5 presented as “< –3.5”.

Label	Reservoir	Validation Outflow		Validation Storage		Reference Outflow		Reference Storage	
		A-HYPE	H-HYPE	A-HYPE	H-HYPE	A-HYPE	H-HYPE	A-HYPE	H-HYPE
a	Abraham Reservoir	–0.048	0.049	< –3.5	0.517	–0.368	–0.190	0.700	0.802
b	Oldman Reservoir	0.395	0.517	< –3.5	0.044	0.347	0.563	–0.595	0.541
c	Lake Diefenbaker	0.419	0.425	0.712	0.717	0.258	0.533	0.702	0.868
d	Tobin Lake	0.375	0.701	< –3.5	–2.03	0.418	0.804	< –3.5	–2.82
e	Cedar Lake	0.134	–0.124	0.377	0.084	0.287	0.153	–0.707	0.078
f	Namakan Lake/Rainy Lake	0.539	0.813	0.634	0.706	0.744	0.917	0.588	0.901
g	Lake of the Woods	0.666	0.724	0.571	0.751	0.829	0.851	0.790	0.889
h	Lake St Joseph	–0.038	–0.298	< –3.5	0.02	–0.061	–0.271	< –3.5	–0.342
		–0.036	–0.261			–0.049	0.435		
i	Lac Seul	0.562	0.528	0.605	0.715	0.467	0.581	0.626	0.720
j	Pointe du Bois Reservoir	0.339	0.735	< –3.5	–0.637	–0.063	0.508	< –3.5	–0.666
k	Rafferty Reservoir	–0.158	0.315	< –3.5	–1.51	–0.035	0.337	–3.23	0.441
l	Lake Manitoba	–0.159	–0.362	0.057	–0.098	–0.089	–0.001	–0.700	–1.27
m	Lake Winnipeg	0.338	0.459	0.590	0.455	0.658	0.776	0.910	0.950
n	Reindeer Lake	0.200	–0.327	–0.549	–0.357	0.345	0.315	0.473	0.872
o	Southern Indian Lake	–0.344	0.015	< –3.5	0.511	–0.251	0.090	< –3.5	0.614
		0.011	0.522			–0.066	0.777		
p	Novosibirskoye	0.573	0.670	N/A	N/A	0.293	0.295	–2.14	0.479
q	Sayano-Shushenskoye	0.512	–0.043	N/A	N/A	–2.95	–1.88	–0.861	–0.005
r	Krasnoyarskoye	–2.24	–3.07	N/A	N/A	–0.795	–0.304	–0.931	–0.438
s	Vilyuyuskoye	–0.164	0.128	N/A	N/A	–0.457	–0.590	0.687	0.617

**Table 5**

Respective optimal percent error of standard deviation for A-HYPE and H-HYPE models for outflow and storage over reference (2001–2010 for Canada, 1991 to 2000 for Russia) and validation (1981–2000 for Canada, 1971 to 1990 for Russia) periods. Validation storage listed as “N/A” for Russian reservoirs due to lack of observed data. Values greater than 100 or less than −100 presented as “> ±100”.

Label	Reservoir	Validation Outflow		Validation Storage		Reference Outflow		Reference Storage	
		A-HYPE	H-HYPE	A-HYPE	H-HYPE	A-HYPE	H-HYPE	A-HYPE	H-HYPE
a	Abraham Reservoir	−77	−68	> ±100	−32	−29	−31	−37	−31
b	Oldman Reservoir	−20	23	> ±100	−8.3	−32	−4.5	20	−47
c	Lake Diefenbaker	−35	−10	−0.45	−22	−40	−17	15	−18
d	Tobin Lake	−34	−6.3	> ±100	19	−34	−4.4	> ±100	70
e	Cedar Lake	−50	−42	−11	−46	−33	−15	36	−18
f	Namakan Lake/Rainy Lake	−2.7	0.32	−11	−42	−6.7	−3.9	19	−10
g	Lake of the Woods	−5.2	−4.6	−0.23	−6.5	−6.1	−6.7	6.3	9.0
h	Lake St Joseph	−71	−48	> ±100	20	−75	−61	> ±100	25
		−91	14			−95	−5.4		
i	Lac Seul	−9	−12	−7.8	−26	−5.0	−19	1	−20
j	Pointe du Bois Reservoir	−44	−23	> ±100	−22	−80	−33	> ±100	−31
k	Rafferty Reservoir	−55	−53	69	44	−62	−58	−5.0	−39
l	Lake Manitoba	−22	−25	−53	−38	5.4	−12	−3.8	17
m	Lake Winnipeg	−19	−24	−30	−25	−4.2	−15	−15	−6.7
n	Reindeer Lake	−56	−26	−22	−33	−46	−37	−21	9.0
o	Southern Indian Lake	−59	−26	> ±100	−8.8	−61	−35	> ±100	0.06
		−87	−3.0			−95	−16		
p	Novosibirskoye	6.1	18	N/A	N/A	−2.4	6.0	> ±100	21
q	Sayano-Shushenskoye	−37	−81	N/A	N/A	79	−4.5	−6.7	−21
r	Krasnoyarskoye	−78	50	N/A	N/A	−11	−19	22	31
s	Vilyuyskoye	−34	−28	N/A	N/A	−9.0	−29	7.1	−14

predictable physically based processes of the environment.

Assessing the optimal NSE performance of reservoir outflow and storage (Table 4, Figs. 7–9), we see an improvement using the H-HYPE regulation. In the reference period, median NSE improves by 0.18 and 0.49 for outflow and storage (where A-HYPE results less than −3.5 are excluded; Figs. 7–9). This reference period (2001–2010 for Canadian and 1991 to 2000 for Russian reservoirs) is where the paired WSL and outflow data are used to develop the parameters and due to the added parameterization of the new routine, improved performance here is expected, as seen in the (lighter shaded region in Figs. 12 and 13). In the validation period, median NSE improvement is by 0.10 and 0.20 for outflow and storage (again, where A-HYPE results less than −3.5 are excluded; Figs. 7–9).

Outflow results improve (by more than +0.1) in 14 and change by a nominal amount ( $\pm 0.1$ ) in four of 21 outlets in the reference period (Fig. 8a and b) and improve in nine and change by a nominal amount in five of 21 outlets in the validation period (Fig. 8c and d). Storage results improve in 14 and change by a nominal amount in four of 19 reservoirs in the reference period (Fig. 9a and b) and improve in 10 and change by a nominal amount in two of 15 reservoirs for the validation period (no validation data available for storage in Russian reservoirs; Fig. 9c and d). Because reservoirs are modelled with observed inflow, there is no spatial pattern to improvements in NSE (Fig. 7 and 8) due to cascading results. Despite a lack of spatial pattern, these show improvement over A-HYPE, with few exceptions.

These results suggest that in the majority of instances, the model is better able to react to interannual (climatic) and intra-annual (i.e., shorter duration floods) variability and correctly apportion water exiting the reservoir seasonally for both the reference and validation historic periods (1981–2010 for Canadian, 1971 to 2000 for Russian reservoirs). It further proves that the storage is better maintained at the seasonal resolution for that same period. Improvements of seasonal storage performance are important to long-term reliability of results and shown to improve in the majority of presented reservoirs. Data availability in this period 1981 to 2000 for Canadian and 1971 to 1990 for Russian reservoirs is more variable, with no WSL data available for the Russian reservoirs in this period. Despite the relative sparsity of observation data and the fact that the regulation rules are derived in the future of these observations have not yet known, performance is still shown to improve using H-HYPE over A-HYPE and in fact shows a greater median

improvement than the reference period.

We further assess changes to the relative error of the standard deviation (RES; Table 5), a component of the Kling-Gupta Efficiency and a practical measure of the simulation skill at replicating sub-weekly reservoir operations or longer-scale climatic variability. The effects of weekly operations can be seen particularly in hydroelectric reservoirs (Déry et al., 2018). The absolute value of RES by using H-HYPE improves by a median of 8.9 and 6.4 percent for outflow and storage, respectively (excluding A-HYPE errors exceeding 100%). These present a reduction of error and therefore a closer approximation of the measured variability. In the validation period, the median change to RES is 7.6 and 15 percent for outflow and storage, respectively (again, excluding A-HYPE errors exceeding 100%). In this sense, the variability of the outflow and storage are improved over AHYPE for both reference and validation periods.

Average annual hydrographs are presented to qualitatively compare A-HYPE and H-HYPE skill at predicting yearly flow regime relative to observations. Each day represents the 30-year average outflow by day of year (reference and validation together). Day of the week is not considered (as seen in Déry et al., 2018) and as such hydro-peaking and statutory holiday effects are generally not visible. These offer an assessment of the skill of the seasonality and sub-seasonal model responses.

Fig. 10 shows an improved seasonality across the majority of reservoirs for outflow. Regardless of the shape of observed outflow seasonality, H-HYPE shows qualitative improvements in dynamic systems with high interannual variability, except in the case of Cedar Lake (Fig. 10e), Lake Manitoba (Fig. 10l), Sayano-Shushenskoye (Fig. 10q), and Krasnoyarskoye (Fig. 10r). This is seen in the case of Lake Manitoba (Fig. 11l) for WSL as well. Sayano-Shushenskoye and Vilyuyskoye have very limited records of overlapping WSL-outflow data (Fig. 1). This limits the ability to parameterize the model based on historic observations.

Notable improvements are shown in Pointe du Bois Reservoir (Figs. 10j and 11j), Rafferty Reservoir (Figs. 10k and 11k), Southern Indian Lake (Fig. 10o1, 10o2, 11o1), and Novosibirskoye (Figs. 10p and 11p) for both outflow and WSL. In the case of Southern Indian Lake (a reservoir with two outlets), improvements are shown in each outlet, leading to improved seasonality in both and as a result: storage. Skill at simulating mean regime over climatic-scale periods (30 years) is important for long-term simulation, but over and above improvements

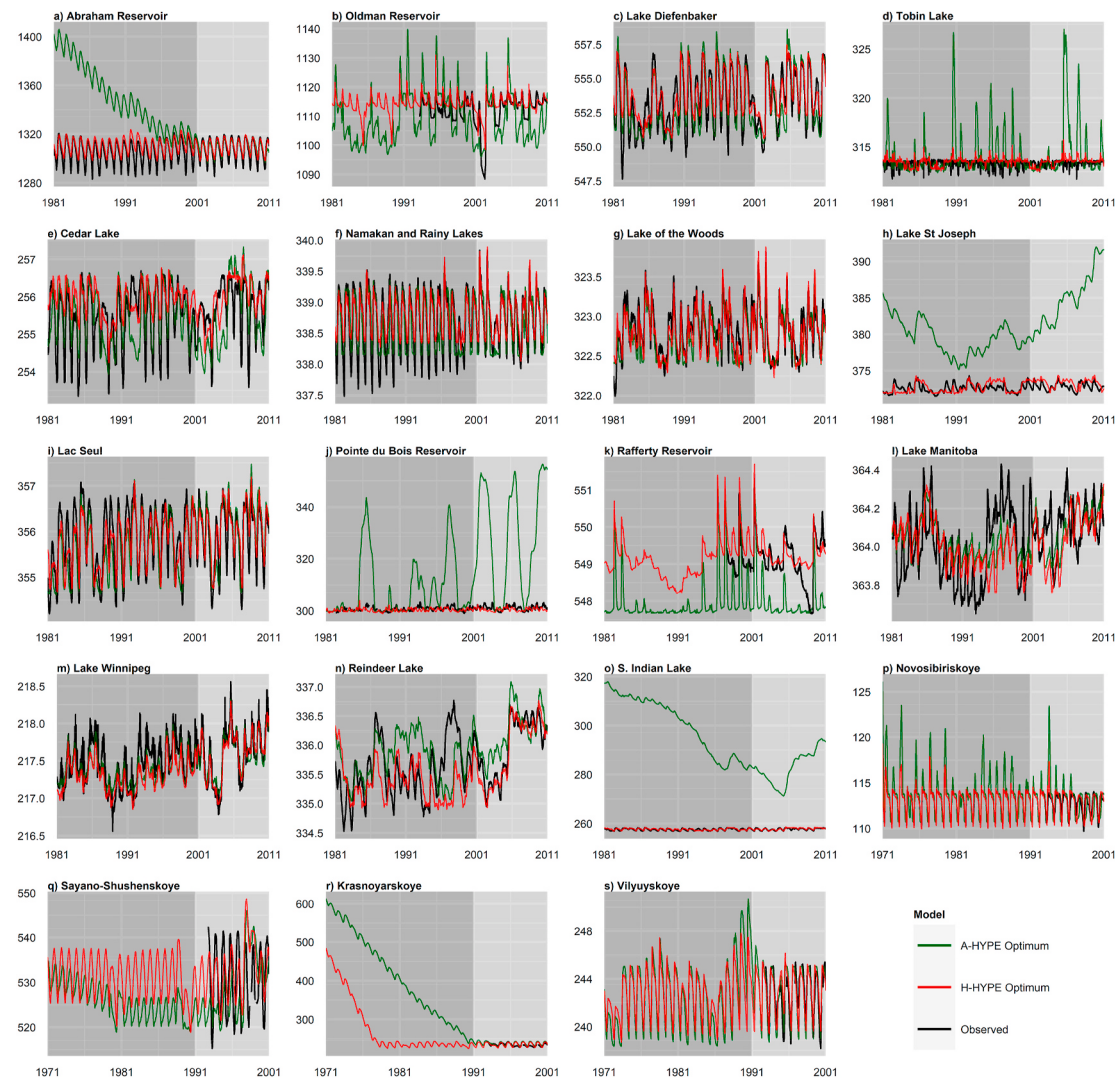


**Fig. 13.** Daily water surface level (all in metres above surface level) for (black) observed, (green) optimal A-HYPE parameters, and (red) optimal H-HYPE parameters. Shaded areas for (dark gray) validation period and (light gray) reference period. Labels correspond to all tables and Fig. 1 and 6 to 13.

to 30-year mean seasonality, skill in daily outflow and WSL is important to examine.

Instances of the most robust hydrograph improvements arise in reservoirs with the greatest interannual variability of water supply (whether by variable inflow or by P/PET ratio; Table 2), such as Lake Diefenbaker (Figs. 10c and 12c) and Oldman Reservoir (Figs. 10b and 11b). This is also seen in reservoirs with less predictable behaviour, such as the hydrograph drawdown operations seen in Lake Winnipeg (August to October; Fig. 10m) or Tobin Lake (May to June; Fig. 10d). Reservoirs with interannual variability in water surface level also show improvement, such as Namakan/Rainy Lake (Figs. 11f and 13f) and Lake of the Woods (Figs. 11g and 13g). In both cases, these reservoirs fail to be as well-represented by the A-HYPE prescribed sine curve (target outflow), but are more accurately captured by H-HYPE, where outflow is more sensitive to daily storage and daily storage is sensitive to an intra-annually variable curve (target storage).

Improvements to performance and the H-HYPE performance itself are more variable in the Russian reservoirs than their Canadian counterparts. Simulation of average storage and storage intra-annual variability are improved by H-HYPE in all Russian reservoirs (Fig. 13p, 13q, 13r, 13s). Outflow performance in Russian reservoirs is improved and greater than 0.5 for Novosibirskoye (Fig. 10p) and improved, though unsatisfactory for Vilyuyeskoye (Fig. 10s). Performance of the Yenisey

river reservoirs' outflow (Fig. 10q, 10r) improve in the reference period (though they are unsatisfactory) and degrade in the validation period. Any improvements to skill are related to the length of synchronous WSL and outflow records (Fig. 1). Distribution of records throughout the year will provide improved parameter estimation over seasonal gauge records. Simulating multiple sets of governing WSLs (which dictate the parameter estimation), a suite of H-HYPE parameter sets is assessed to determine the optimal formulation for each reservoir. In the case of the Russian reservoirs, the period of overlap is much shorter (greater than 1 full year, but generally less than 4, where the Canadian records are closer to the full 10-year reference period). The WSL records of Russian reservoirs are derived from a 10-day satellite pass, which will also account for consistent gaps in the records. The poor performance in the validation period of the Russian discharge stations is also due to three of the four stations being commissioned (Sayano-Shushenskoye: 1985, Krasnoyarskoye: 1972, and Vilyuyeskoye: 1973; Table 1) in the validation period (i.e., the outflow was natural until then; Fig. 12q, 12r, 12s). This is particularly of note in Krasnoyarskoye (Figs. 10r, 11r and 12r, and 13r), where the regulated outflow is capped at its fixed maximum while the outflow reaches naturalistic peaks.

## 5. Study limitations

### 5.1. Basin similarities and reservoir discontinuity

The RAT and the regulation routine in H-HYPE should continue to be tested in basins of different climatic conditions and basins with different inter-reservoir connectivity (i.e., series of cascading reservoirs, parallel reservoirs) to assess its applicability in modelling at different time and spatial scales. These reservoirs are tested in isolation, using observed inflow records to ‘nudge’ the hydrologic model in largely nival basins. A study of basin-wide sensitivity to the propagation of improved or degraded simulation performance would be useful in determining the degree of upstream effect of each reservoir. Studies using remote sensing to determine WSLs show increasing promise for integrated operational modelling (Mehran et al., 2017; Revilla-Romero et al., 2016) as well as more detailed depth-surface area modelling rather than as a rectangular prism (more accurate than keeping surface area fixed; Shin et al., 2019). While less impressive than the gauged counterparts, reservoirs with satellite WSL records (Russian reservoirs, courtesy of G-REALM) are shown to function in H-HYPE. Treating these results as improving on those available through current A-HYPE, the RAT should be coupled with remote sensing to further test applicability in even more remote areas, such as throughout the Arctic in A-HYPE.

### 5.2. Regulation stationarity

This work holds regulation rules and infrastructure presence constant. Constant infrastructure assumes that no new control structures will be brought online through 2070, which is already questionable given the construction of the Keeyask generating station in the NCRB, with a commissioning date in late 2020. This study omits existing regulation points in the basins examined, due to record availability (such as three reservoirs or generating station forebays on the Lower Nelson River generation complex in the NCRB and four reservoirs on the Angara river downstream of Lake Baikal). The regulated system model assumes an ‘energy future’ consistent with today’s power demand and energy production (no alteration to operations). This further assumes the daily target WSLs (selected from the reference period) will not change. Flood and drought stages of reservoirs rarely change as they would require costly infrastructure redesign. The extent of the operations stages within the safe limits (flood to drought) are tied to the seasonality of power demand, but by no means stationary. Although the seasonality of the operations zone is unlikely to change, the depth of the zone and its location relative to flood and drought stages easily could. As noted by Nazemi and Wheater (2015b), future studies should examine a “a systematic scheme for dealing with non-stationary parametric estimation” or a method examining changing flow regimes (such as inflow or temperature, as in Solander et al., 2016) to change the rules used to govern regulation. This could be achieved by using the RAT to develop different regulation rules from different reference periods, updated periodically in multi-decade simulations.

### 5.3. Fixed parameter sets and full optimization

Though this method offers more flexibility in the type of outflow used by zone (monthly storage-outflow, storage-based, etc.), it carries the associated burden of much higher dimensionality if the historic least-squares relationships are to be improved upon by means of a true optimization. This progression beyond a “generalized parameter set” has been shown by Yassin et al. (2019) to offer largest improvements in those reservoirs with the lowest base performance. This optimization could improve those reservoirs currently underperforming (e.g. Reindeer Lake) relative to A-HYPE. A full examination of a calibrated parameterization (rather than deriving a generalized set based on historic data) would further illuminate parametric uncertainty in the model and could be useful in examining the identifiability of both free

(storage-outflow coefficients and exponents) and integer (zone-option flag) parameters.

## 6. Conclusions

The new regulation routine presented herein is applicable to many types of reservoirs or operational schemes and presents more robust results relative to the default regulation routines available in HYPE (i.e., A-HYPE). This synthesis of numerous processes modelled in other macroscale regulation routines, as well as the offline analysis system fulfill objectives of (1) and (2) outlined in the introduction (Section 1.1). By presenting a methodology for automated determination of regulated reservoir stage and outflow relationships used in HYPE (though applicable to any hydrologic model), this work presents a possible solution to an ongoing question in continental- and global-scale hydrologic modelling: “A general problem with modelling river regulation is that reservoirs can have multiple purposes and must be examined individually” (Arheimer et al., 2020). At a global scale, the recent Worldwide-HYPE model employs 2500 regulated reservoirs (Arheimer et al., 2020). By presenting a viable workflow to parameterize reservoirs using openly available observed records, this work hopes to address a need for a method to systematically assess point-scale reservoir operations which cumulatively affect the continental to global scale hydrologic cycle in semi-distributed hydrologic models.

The value of this model is proven by examining the results from 15 reservoirs within western Canada and four spread across Russian rivers. These span snow-fed hydroelectric plants in the Rocky Mountains to semi-arid Canadian Prairie water-supply reservoirs, running the gamut of average daily throughput from  $2.5 \text{ m}^3\text{s}^{-1}$  in the Canadian Prairies to  $2500 \text{ m}^3\text{s}^{-1}$  in the largest rivers of Siberia. An advantage of the H-HYPE regulation routine is that it can be structured as simple as necessary or as complex as data-availability allows. Physical parameters are derived based on historic observations (as in Yassin et al., 2019) and tested for hundreds of combinations of the WSLs governing the zones and parameter derivation using the reservoir analysis tool before inclusion in the larger hydrological model and shown to avoid equifinality with few exceptions.

Simulated outflows from the new H-HYPE dam routine generally improve upon those simulated by the existing A-HYPE dam routine. This is reflected in the statistical improvement of the long-term seasonal regulated outflows and when comparing individual seasons, where the H-HYPE routine better adjusts to intra-annual (storm-flood events) and interannual (prolonged floods and droughts) hydro-climatic periods in a manner more consistent with the observed record for historic 20-year periods, using rules derived from more recent 10-year periods. The improvement of H-HYPE over A-HYPE is proven in eight locations in the Canadian Prairies, cited as problem area in previous studies of regulation modelling (Amir Jabbari and Nazemi, 2019). The majority of results also show improvement in storage, proving the routine’s ability to simultaneously simulate inter-connected elements of reservoir regulation, addressing objective (3) of in the introduction.

Further investigation of multiple parameter sets would be of interest in quantifying uncertainty, but in estimating parameter sets we prove the utility of this routine and the reservoir analysis tool in simulating reservoir outflow and storage for 19 reservoirs in Canada and Russia, over 30-year periods. This employs a methodology which systematically tests multiple combinations of the formulation of a piecewise equation and multiple thresholds of that piecewise equation to replicate simple (run-of-the-river hydroelectric plants), complex (interannually variant or seasonally ice-covered), and multi-use (multiple operations goals dependant on seasonal or annual wetness) reservoir operations. In doing so, improvements are made in the simulation of processes which, while regulated, are often chaotic or tied to human judgement.

## Declaration of interest

This work was undertaken as part of a series of projects (BaySys; Barber, 2014) including collaboration with Manitoba Hydro, University of Manitoba, and supported in part by the Natural Sciences and Engineering Research Council of Canada (NSERC). NSERC funding was provided as part of the funding to BaySys under CRD number 477028-14. Manitoba Hydro interest (in development of study scope and focus) was limited to provision of internal reports summarizing reservoir regulation, access to extended streamflow and water surface level records, and access to in-house reservoir regulation model code used in developing governing algorithms. No limitations on research scope or focus were imposed and contributions are limited to those noted in-text.

## Contributions of Co-Authors

Dr. MacDonald was instrumental in the prior development of the Hudson Bay HYPE (H-HYPE) model, the Hydrological Predictions for the Environment (HYPE) sub-model developed specifically for this project through his work with the Swedish Meteorological and Hydrological Institute (SMHI). Dr. Stadnyk provided guidance on project scope and the editing of the manuscript. Kristina Koenig and Phil Slota provided industrial knowledge related to the Nelson-Churchill River Basin and the Manitoba Hydro regulated system as well as high-level guidance on reservoirs selected for regulation in hydrologic modelling. John Crawford developed the original Cedar Lake, Lake Winnipeg, SIL, Lake of the

Woods/Namakan Lake/Rainy Lake, and Lake St. Joseph/Lac Seul spreadsheet models. Phil Slota developed the original Reindeer Lake spreadsheet model. John Crawford was the primary developer of the ideal storage method used in the H-HYPE regulation routine and designed the reservoir-specific sub-functions of the spreadsheet models. Some of these sub-functions in the spreadsheet models would later be modified, adapted, and aggregated to form the basis of the reservoir analysis tool (RAT) and the H-HYPE regulation routine. Matthew Hamilton aided in the coding of the HYPE regulation routine used in this work. All authors contributed to the editing of the manuscript text.

## Declaration of competing interest

The authors declare that they have no known competing financial interests or personal relationships that could have appeared to influence the work reported in this paper.

## Acknowledgements

Thanks to University of Manitoba, Manitoba Hydro and partners funding through the Natural Sciences and Engineering Research Council of Canada through funding of the BaySys project. Many thanks to Manitoba Hydro for technical and logistical support of regulation system modelling. Many thanks to the Water Survey of Canada (WSC), Global Runoff Data Centre (GRDC), and the Global Reservoirs and Lakes Monitor (G-REALM) for the gathering and dissemination of discharge and WSL data.

## Appendix A. : H-HYPE and A-HYPE governing equations

**Table A1**

H-HYPE governing equations. Equation numbers correspond to Figs. 3 and 4. Symbol “ $\theta$ ” indicates a parameter derived using the Reservoir Analysis Tool (RAT) from historic records summarized in Table A3.

#	Where	Equation
A-1	No Conditions	$WSL_{op-i} = \frac{(DOY_i - fDOY_j) \times (\theta_{WSL,avg,j+1} - \theta_{WSL,avg,j})}{(fDOY_{j+1} - fDOY_j)} + \theta_{WSL,avg,j} - \frac{\theta_{opDepth}}{2}$
A-2	No Conditions	$WSL_{op+i} = \frac{(DOY_i - fDOY_j) \times (\theta_{WSL,avg,j+1} - \theta_{WSL,avg,j})}{(fDOY_{j+1} - fDOY_j)} + \theta_{WSL,avg,j} + \frac{\theta_{opDepth}}{2}$
A-3	No Conditions	$WSL_{tr-i} = WSL_{op-i} - \theta_{transDepth}$
A-4	No Conditions	$WSL_{tr+i} = WSL_{op+i} + \theta_{transDepth}$
A-5	No Conditions	$WSL_{dr} = \theta_{WSL,dr}$
A-6	No Conditions	$WSL_{fl} = \theta_{WSL,fl}$
A-7	No Conditions	$WSL_{i+1} = WSL_i + \frac{86400 \times (\sum Q_{in,i} - \sum Q_{out,i})}{SA \times 10^6} + \frac{(P_i - ET_i)}{10^3}$

Equations A-1 through A-6 compute daily threshold stages for day  $i$  describing the seven zones used to determine reservoir outflow. Drought and flood stages ( $WSL_{fl}$ ,  $WSL_{dr}$  [m]) are fixed values ( $\theta_{WSL,dr}$ ,  $\theta_{WSL,fl}$  [m]). Daily upper and lower bounds of the operations zone ( $WSL_{op+i}$ ,  $WSL_{op-i}$  [m]) are computed daily using the target stage ( $\theta_{WSL,avg,j}$  [m]) for the first day ( $fDOY$  [day]) of month  $j$ , the current day of year  $DOY_i$ , and the depth of the operations zone ( $\theta_{opDepth}$  [m]). The upper and lower extents of the transition zones ( $WSL_{tr+}$ ,  $WSL_{tr-}$  [m]) are specified by the day's operations depths and the depth of the transition zones ( $\theta_{transDepth}$  [m]). The current timestep's total inflow ( $Q_{in,i-1}$  [ $m^3 s^{-1}$ ]), computed total outflow ( $Q_{out,i}$  [ $m^3 s^{-1}$ ]), WSL ( $WSL_i$  [m]), precipitation and evaporation off of the lake surface ( $P_i$ ,  $ET_i$  [mm]) and the reservoir surface area ( $SA$  [ $km^2$ ]) are used to determine the next timestep's WSL, as described by Equation A-7. These equations are executed for timestep.

#	Where	Equation
A-8	$WSL_{dr} \leq WSL_i \leq WSL_{tr-i}$	$Q_{low,i} = \theta_{fixedA,lo} \times (WSL_i - WSL_{dr})^{\theta_{fixedB,lo}}$
A-9	$WSL_{op-i} \leq WSL_i \leq WSL_{op+i}$	$Q_{op,i} = \theta_{fixedA,op} \times (WSL_i - MIN[WSL_{op-}])^{\theta_{fixedB,op}}$
A-10	$WSL_{tr+i} \leq WSL_i \leq WSL_{fl}$	$Q_{hi,i} = \theta_{fixedA,hi} \times (WSL_i - MIN[WSL_{op+}])^{\theta_{fixedB,hi}}$

Equations A-8, A-9, and A-10 compute daily outflow based on a single, year-round storage-outflow curve (“Fixed Curve” in Fig. 3, Table 3). This curve relates the daily WSL ( $WSL_i$  [m]) to the outflow using two parameters ( $\theta_{fixedA,stage}$ ,  $\theta_{fixedB,stage}$  for each of the low, operations, and high zones) and the depth above the bottom of the current zone ( $WSL_{dr}$ ,  $MIN[WSL_{op-}]$ , or  $MIN[WSL_{op+}]$ ). Where the bottom of a zone varies throughout the year, the stage depth is computed relative to the minimum ( $MIN[WSL_{stage}]$ ). It is effectively used to mimic a known relationship (i.e., turbine efficiency vs. reservoir level, spillway geometry, weir equations, etc.). These computations are executed at each timestep, but only when the stage options ( $\varphi_{lo}$ ,  $\varphi_{op}$  or  $\varphi_{hi}$ ) for the relevant stages are set

to the “Fixed Curve” flag value for the primary or secondary outlet (this is the case for all high stages for primary outlets).

#	Where	Equation
A-11	$WSL_{dr} \leq WSL_i \leq WSL_{tr-i}$	$Q_{lo,j} = \theta_{monthly,lo,j} \times (WSL_i - WSL_{dr})$
A-12	$WSL_{dr} \leq WSL_i \leq WSL_{tr-i}$	$Q_{lo,i} = Q_{lo,j} \times \omega_{ij} + Q_{lo,j-1} \times (1 - \omega_{ij})$
A-13	$WSL_{op-i} \leq WSL_i \leq WSL_{op+i}$	$Q_{lo,base,j} = \theta_{monthly,lo,j} \times (\text{MIN}[WSL_{op-j}] - WSL_{dr})$
A-14	$WSL_{op-i} \leq WSL_i \leq WSL_{op+i}$	$Q_{op,j} = \theta_{monthly,op,j} \times (WSL_i - \text{MIN}[WSL_{op-j}]) + Q_{lo,base,i}$
A-15	$WSL_{op-i} \leq WSL_i \leq WSL_{op+i}$	$Q_{op,i} = Q_{op,j} \times \omega_{ij} + Q_{op,j-1} \times (1 - \omega_{ij})$
A-16	$DOM_i \leq 15$	$\omega_{ij} = 0.5 - \frac{DOM_i}{30.5}$
A-17	$DOM_i > 15$	$\omega_{ij} = 1.5 - \frac{DOM_i}{30.5}$

Equations A-11 through A-15 compute daily outflow based on linear monthly storage-outflow relationships (“Monthly” in Fig. 3, Table 3). Equations A-16 and A-17 determines the current day of month’s ( $DOM_i$ ) weight between the midpoints of the current month and the next month ( $\omega_{ij}$ ). This curve relates the daily WSL ( $WSL_i$  [m]) to the outflow using monthly parameters ( $\theta_{monthly,stage,j}$  for each of the low and operations zones), the depth above the bottom of the current zone, for the current month ( $WSL_{dr}$  or  $\text{MIN}[WSL_{op-j}]$ ). The operations zone outflow includes the maximum low zone outflow ( $Q_{lo,base,j}$ ) as if they form a compound pair of linear relationships. This is used to replicate seasonally variant operations (i.e., increased or decreased hydroelectric demand, modified hydraulics based on ice-cover, etc.) while bypassing manual calibration. These computations are executed at each timestep, but only when the stage options ( $\varphi_{lo}$  or  $\varphi_{op}$ ) for the relevant stages are set to the “Monthly” flag value for the primary or secondary outlet.

#	Where	Equation
A-18	$WSL_i \leq WSL_{dr,i}$	$Q_{dr,i} = \theta_{Q,dr}$
A-19	$WSL_i \leq WSL_{fl,i}$	$Q_{fl,i} = \theta_{Q,fl}$

Equations A-18 and A-19 compute fixed daily outflow (“Fixed” in Fig. 3, Table 3 for drought and flood, respectively). Values are computed based on extrema within historical records ( $\theta_{dr}$ ,  $\theta_{fl}$ ). These values reproduce operations for specified ecological minima or the allowable downstream maxima. These computations are executed at each timestep, but only when the stage options ( $\varphi_{dr}$  or  $\varphi_{fl}$ ) for the relevant stages are set to the “Fixed Value” flag value for the primary or secondary outlet (this is the case for all drought stages).

#	Where	Equation
A-20	No Conditions	$Q_{fl,i} = Q_{hi,i}$

Equation 20 computes flood zone outflow where high zone operations are extended (“Extend High” in Fig. 3, Table 3). Since high zone outflow is sensitive to daily level ( $WSL_i$ ), extending the high zone to flood zone equations results in flood zone outflows intensifying to relieve over-burdened reservoirs, which is consistent with real-world operations. These computations are executed at each timestep, but only when the flood option ( $\varphi_{fl}$ ) is set to the “Extend High” flag value for the primary or secondary outlet.

#	Where	Equation
A-21	No Conditions	$Q_{op,i} = (1 + \theta_i) \times \frac{\sum_{i=13}^i Q_{in,i}}{14} + \frac{SA \times 10^6}{86400} \times \left( \frac{\sum_{i=13}^i \Delta S_{avg,i}}{14} \right)$
A-22	No Conditions	$\Delta S_{avg,i} = (WSL_{op-i} - WSL_{op-i+1})$
A-23	$WSL_i \leq WSL_{tr-i}$	$\theta_i = -0.25$
A-24	$WSL_{tr-i} \leq WSL_i \leq WSL_{avg,i}$	$\theta_i = -0.25 \times \frac{(WSL_i - (WSL_{op-i} + \theta_{op+depth}))}{(WSL_{tr+i} - (WSL_{op-i} + \theta_{op+depth}))}$
A-25	$WSL_{avg,i} \leq WSL_i \leq WSL_{tr+i}$	$\theta_i = 0.25 \times \frac{(WSL_i - (WSL_{op-i} + \theta_{op+depth}))}{(WSL_{tr+i} - (WSL_{op-i} + \theta_{op+depth}))}$
A-26	$WSL_{tr+i} \leq WSL_i$	$\theta_i = 0.25$

Equations A-21 through A-26 are used to determine the daily outflow based on the ideal daily storage (operations zone for primary outlets only, “Ideal Storage” in Fig. 3, Table 3). This method calculates the outflow necessary to reach daily target storage ( $WSL_{avg,i}$ ), based on the previous two weeks’ average inflow and the gradient of the target WSL curve. This option is employed in reservoirs with limited overlapping outflow and WSL records (which prevents development of monthly or year-round relationships). This method was proposed by John Crawford for Manitoba Hydro for historic and projected simulation of operations. This method maintains operations zone WSLs very efficiently. These computations are executed at each timestep, but only when the operations option ( $\varphi_{op}$ ) is set to the “Ideal Storage” flag value for the primary outlet.

#	Where	Equation
A-27	No Conditions	$Q_{hi,avg,i} = \frac{\sum_{i=1}^{i=7} Q_{in}}{7}$
A-28	No Conditions	$Q_{out,primary,avg,i} = \frac{\sum_{i=1}^{i=7} Q_{out,primary}}{7}$
A-29	No Conditions	$Q_{hi,i} = Q_{in,avg,i} - Q_{out,primary,avg,i}$

Equations A-27, A-28, and A-29 compute daily outflow to prevent flooding in a two-outlet reservoir (high zone for secondary outlets only, also called “Ideal Storage” in Fig. 3, Table 3). This method uses a seven-day inflow gradient to respond to shorter, more intense high-inflow events. This option is used to simulate secondary outlets where the secondary outlet flow is not heavily governed but used to protect reservoir storage or safe levels. The two “Ideal Storage” options can only be applied to separate zones and separate outlets because in development, they made the model unstable if jointly applied. These computations are executed at each timestep, but only when the high option ( $\varphi_h$ ) is set to the “Ideal Storage” flag value for the secondary outlet.

#	Where	Equation
A-30	No Conditions	$Q_{cond,avg,i} = \frac{\sum_{i=1}^{i=14} Q_{cond}}{14}$
A-31	$WSL_{dr} \leq WSL_i \leq WSL_{fl}$	$Q_{op,i} = \theta_{A,cond} \times (Q_{cond,avg,i} - \theta_{B,cond})^{\theta_{C,cond}} + \theta_{D,cond}$

Equations A-30 and A-31 compute daily outflow based on the discharge at another sub-basin within the model (operations zone for main outlet only; “Condition” in Fig. 3, Table 3). This option is used where the outflow of a reservoir needs to be limited or increased based on conditions at another gauge station. This method uses a four-parameter curve ( $\theta_{A,cond}$ ,  $\theta_{B,cond}$ ,  $\theta_{C,cond}$  and  $\theta_{D,cond}$ ) to relate the calculated outflow for a reservoir to another sub-basin’s previous two weeks’ outflow. The application of a conditioned outflow can be automatically selected by the RAT but will only create feasible values if a corresponding record (or simulated point in H-HYPE) is present, which pre-supposes a degree of understanding of the regulated system. These computations are executed at each timestep, but only when the high option ( $\varphi_{op}$ ) is set to the “Condition” flag value for the primary outlet.

#	Where	Equation
A-32	$Q_{lo,i} < Q_{dr,i}$	$Q_{lo,i} = Q_{dr,i}$
A-33	$Q_{lo,i} > Q_{fl,i}$	$Q_{lo,i} = Q_{fl,i}$
A-34	$Q_{hi,i} > Q_{fl,i}$	$Q_{hi,i} = Q_{fl,i}$
A-35	$Q_{hi,i} < Q_{dr,i}$	$Q_{hi,i} = Q_{dr,i}$
A-36	$Q_{op,i} < Q_{lo,i}$	$Q_{op,i} = Q_{lo,i}$
A-37	$Q_{op,i} > Q_{hi,i}$	$Q_{op,i} = Q_{hi,i}$
A-38	No Conditions	$Q_{tr-,i} = Q_{lo,i} + \frac{(Q_{op,i} - Q_{lo,i})(WSL_i - WSL_{tr-,i})}{(WSL_{op-,i} - WSL_{tr-,i})}$ $Q_{tr+,i} = Q_{op,i} + \frac{(Q_{hi,i} - Q_{op,i})(WSL_i - WSL_{op+,i})}{(WSL_{tr+,i} - WSL_{op+,i})}$
A-39	No Conditions	
A-40	$WSL_i \leq WSL_{dr,i}$	$Q_{dec,i} = Q_{dr,i}$
A-41	$WSL_{dr,i} \leq WSL_i \leq WSL_{tr-,i}$	$Q_{dec,i} = Q_{low,i}$
A-42	$WSL_{tr-,i} \leq WSL_i \leq WSL_{op-,i}$	$Q_{dec,i} = Q_{tr-,i}$
A-43	$WSL_{op-,i} \leq WSL_i \leq WSL_{op+,i}$	$Q_{dec,i} = Q_{op,i}$
A-44	$WSL_{op+,i} \leq WSL_i \leq WSL_{tr+,i}$	$Q_{dec,i} = Q_{tr+,i}$
A-45	$WSL_{tr+,i} \leq WSL_i \leq WSL_{fl,i}$	$Q_{dec,i} = Q_{hi,i}$
A-46	$WSL_{fl,i} \leq WSL_i$	$Q_{dec,i} = Q_{fl,i}$
A-47	$(Q_{dec,i} - Q_{out,i-1}) > \theta_{\Delta Q}$	$Q_{out,i} = Q_{out,i-1} + \theta_{\Delta Q}$
A-48	$(Q_{dec,i} - Q_{out,i-1}) < -\theta_{\Delta Q}$	$Q_{out,i} = Q_{out,i-1} - \theta_{\Delta Q}$

Equations A-32 through A-37 run logical corrections. Equations A-38 and A-39 compute transition flow between low and operations zones ( $Q_{tr-,i}$ ) and operations and high zones ( $Q_{tr+,i}$ ) based linear interpolation between corrected zonal flows ( $Q_{lo,i}$ ,  $Q_{op,i}$  and  $Q_{hi,i}$ ), zone stages ( $WSL_{tr-,i}$ ,  $WSL_{tr+,i}$ ,  $WSL_{op-,i}$  and  $WSL_{op+,i}$ ) and daily computed WSL (WSL<sub>i</sub>) to smooth transitions between operational types. Equations A-40 through A-46 determine the selected outflow for the given outlet (primary or secondary  $Q_{dec,i}$ ) based on the current timestep’s WSL (WSL<sub>i</sub>) and the stages separating zones ( $WSL_{dr}$ ,  $WSL_{tr-,i}$ ,  $WSL_{tr+,i}$ ,  $WSL_{op-,i}$ ,  $WSL_{op+,i}$ ,  $WSL_{fl}$ ). Equations A-47 and A-48 restrict daily changes to outflow based on the historical maximum daily change ( $\theta_{\Delta Q}$ ). These operational restrictions, limit maximum change of outflow between two timesteps and are used to simulate operations which might limit potential damage to reservoir infrastructure or downstream municipalities from dramatic changes (i.e., riverbed scour, flash flooding, wildlife isolation), and are computed from historic records 2001 to 2010.

**Table A3**

Source of inflow, outflow, and water surface level datasets by reservoir. Database data listed as “Synthetic” are computed as summarized in Section 3.3. Period indicates gauged years used in this work. Alterations to gauged data: “Unaltered”: gauges exist at the inlet/outlet of a reservoir (or gauged drainage area is within  $\pm 1\%$  of reservoir drainage area), “Scaled Up”/“Scaled Down”: gauged data are scaled directly by the ratio of gauged and reservoir drainage areas.

Label	Reservoir	River	Data	ID (Database)	Period	Alteration	Reference
a	Abraham Reservoir	N/A	WSL	05DC009 (WSC)	1972–2012	Unaltered	—
		N. Saskatchewan River	Qout	05DC007 (WSC)	1953–1968	Unaltered	—
		N. Saskatchewan River	Qin	05DC010 (WSC)	1972–2015	Scaled Up	—
b	Oldman Reservoir	N/A	WSL	05AA032 (WSC)	1992–2015	Unaltered	—
		Oldman River	Qout	05AA023 (WSC)	1949–2008	Scaled Down	—
		Oldman River	Qin	05AA035 (WSC)	2009–2015	Scaled Up	—
c	Lake Diefenbaker	Oldman River	Qin	Synthetic	1981–2008	N/A	—
		N/A	WSL	05HF003 (WSC)	1964–2015	Unaltered	<a href="#">Shook and Pomeroy, (2016)</a>
d	Tobin Lake	S. Saskatchewan River	Qout	05HG001 (WSC)	1911–2015	Scaled Down	—
		Total Inflow	Qin	Synthetic	1981–2015	N/A	—
		N/A	WSL	05KD004 (WSC)	1962–2015	Unaltered	—
e	Cedar Lake	Saskatchewan River	Qout	05KD003 (WSC)	1962–2015	Scaled Down	—
		Total Inflow	Qin	Synthetic	1981–2015	N/A	—
		N/A	WSL	05KL005 (WSC)	1940–2014	Unaltered	—
f	Namakan/Rainy Lake	Saskatchewan River	Qout	05KL001 (WSC)	1909–2014	Unaltered	—
		Saskatchewan River	Qin	05KJ001 (WSC)	1913–2016	Scaled Up	—
		N/A	WSL	05PB007 (WSC)	1911–2015	Unaltered	<a href="#">“Lake of the Woods ...” (2006) LWCB</a>
		N/A	WSL	05PA003 (WSC)	1912–2007	Unaltered	—
		Rainy River	Qout	05PC019 (WSC)	1905–2015	Unaltered	—
		Seine River	Qin	05PB009 (WSC)	1963–2015	Scaled Up	—
g	Lake of the Woods	Turtle River	Qin	05PB014 (WSC)	1914–2015	Scaled Up	—
		Namakan River	Qin	05PA006 (WSC)	1921–2015	Scaled Up	—
		N/A	WSL	05PE012 (WSC)	1913–2015	Unaltered	<a href="#">“Lake of the Woods ...” (2006) LWCB</a>
		Winnipeg River E. Outlet	Qout	05PE006 (WSC)	1907–2015	Unaltered	—
		Winnipeg River W. Outlet	Qout	05PE011 (WSC)	1913–2015	Unaltered	—
h	Lake St. Joseph	Rainy River	Qin	05PC018 (WSC)	1928–2015	Scaled Up	—
		N/A	WSL	05GA004 (WSC)	1934–1994	Unaltered	<a href="#">“Lake of the Woods ...” (2006) LWCB</a>
		Albany River	Qout	04GA001 (WSC)	1968–1994	Unaltered	—
		Albany River	Qout	04GC002 (WSC)	1970–2015	Scaled Down	—
		Albany River	Qout	Synthetic	1994–2006	N/A	—
		Root River	Qout	05QB006 (WSC)	1957–1994	Unaltered	—
		Root River	Qout	Synthetic	1994–2010	N/A	—
i	Lac Seul	Cat River	Qin	04GA002 (WSC)	1970–2015	Unaltered	—
		N/A	WSL	05QB003 (WSC)	1917–2015	Unaltered	<a href="#">“Lake of the Woods ...” (2006) LWCB</a>
		English River	Qout	05QE006 (WSC)	1907–1994	Unaltered	—
		Root River	Qin	—	1957–1994	Unaltered	—

(continued on next page)

**Table A3 (continued)**

Label	Reservoir	River	Data	ID (Database)	Period	Alteration	Reference
j	Pointe du Bois Reservoir	Total Inflow	Qin	05QB006 (WSC)	1981–2010	N/A	—
		N/A	WSL	05PF051 (WSC)	1928–2015	N/A	—
		Winnipeg River	Qout	05PF063 (WSC)	1907–2015	Scaled Down	—
		English River	Qin	05QE005 (WSC)	1927–1994	Unaltered	—
		Winnipeg River	Qin	05PE020 (WSC)	1892–2010	Unaltered	—
k	Rafferty Reservoir	Winnipeg and English Rivers	Qin	Synthetic	1994–2015	N/A	—
		N/A	WSL	05NB032 (WSC)	1991–2015	Unaltered	—
		Souris River	Qout	05NB036 (WSC)	1992–2015	Unaltered	—
l	Lake Manitoba	Souris River	Qin	05NB017 (WSC)	1959–2011	Scaled Up	—
		N/A	WSL	05LK002 (WSC)	1923–2015	Unaltered	—
		Fairford River	Qout	05LM001 (WSC)	1912–2015	Unaltered	—
		Waterhen River	Qin	05LH005 (WSC)	1950–2015	Unaltered	—
		Whitemud River	Qin	05LL002 (WSC)	1971–2015	Scaled Up	—
m	Lake Winnipeg	Portage Diversion	Qin	05LL019 (WSC)	1970–2015	Unaltered	—
		N/A	WSL	05RE003 (WSC)	1983–2015	Unaltered	“Water Power Licences ...” (2010) Manitoba Hydro; “Lake Winnipeg Regulation” (2014 a-g) Manitoba Hydro
		Nelson River E. Channel	Qout	05UB008 (WSC)	1967–2014	Scaled Down	—
		Nelson River Jenpeg	Qout	05UB009 (WSC)	1975–2014	Scaled Down	—
		Dauphin River	Qin	05LM006 (WSC)	1077–2015	Unaltered	—
		Saskatchewan River	Qin	05KL001 (WSC)	1909–2014	Unaltered	—
		Winnipeg River	Qin	05PF063 (WSC)	1907–2014	Scaled Up	—
		Red River	Qin	05OJ010 (WSC)	1962–2008	Scaled Up	—
		Pigeon River	Qin	05RD008 (WSC)	1957–1996	Scaled Up	—
		Beren's River	Qin	05RD007 (WSC)	1957–1992	Scaled Up	—
		Poplar River	Qin	05RE001 (WSC)	1967–1996	Scaled Up	—
n	Reindeer Lake	Total Inflow	Qin	Synthetic	1981–2014	N/A	—
		N/A	WSL	06DB001 (WSC)	1930–2015	Unaltered	—
		Reindeer River	Qout	06DD002 (WSC)	1985–2015	Unaltered	—
		Reindeer River	Qout	06DB002 (WSC)	1929–1987	Unaltered	—
		Cochrane River	Qin	06DA002 (WSC)	1968–2015	Scaled Up	—
o	Southern Indian Lake	Wathaman River	Qin	06DC001 (WSC)	1071–2015	Scaled Up	—
		N/A	WSL	06EC001 (WSC)	1956–2015	Unaltered	“Regional ...” (2015) Manitoba Hydro; “Water Power ...” (1973) Province of Manitoba; “Final Licence ...” (1975) Province of Manitoba; “Water Power ...” (2018) Province of Manitoba
		Churchill River	Qin	06EB004 (WSC)	1973–2015	Scaled Up	—
		Churchill River	Qout	06FB001 (WSC)	1960–2015	Scaled Down	—
		Gauer River	Qout	06FA001 (WSC)	1979–2015	Scaled Down	—
		S. Channel Diversion	Qout	06EC002 (WSC)	1993–2010	Unaltered	—
		S. Channel Diversion	Qout	Synthetic	1981–1992	N/A	—
p	Novosibiriskoye	N/A	WSL	1378 (G-REALM)	1992–2003	Unaltered	—
		N/A	WSL		2008–2019	Unaltered	—

(continued on next page)

**Table A3 (continued)**

Label	Reservoir	River	Data	ID (Database)	Period	Alteration	Reference
q	Sayano-Shushenskoye	Ob River	Qout	2910605 (GRDC)	1958–2000	Scaled Down	
		Karakan River	Qin	2910635 (GRDC)	1956–1998	Scaled Up	
		Berd River	Qin	2910650 (GRDC)	1956–2000	Scaled Up	
		Ob River	Qin	2910606 (GRDC)	1936–2000	Scaled Up	
		Total Inflow	Qin	Synthetic	1998–2010	N/A	
		N/A	WSL	0459 (G-REALM)	2008–2019	Unaltered	—
		Yenisey	Qout	2909158 (GRDC)	1911–1999	Scaled Down	
		Us	Qin	2909250 (GRDC)	1951–1999	Scaled Up	
		Yenisey	Qin	2909160 (GRDC)	1926–2015	Scaled Up	
		Khemchik	Qin	2909240 (GRDC)	1975–1993	Scaled Up	
		Kantegir	Qin	2909313 (GRDC)	1979–1993	Scaled Up	
r	Krasnoyarskoye	Total Inflow	Qin	Synthetic	1993–2010	N/A	
		N/A	WSL	0425 (G-REALM)	1992–2019	Unaltered	—
		Yenisey	Qout	2909156 (GRDC)	1955–1999	Scaled Down	
		Abakan	Qin	2909260 (GRDC)	1953–2015	Scaled Up	
		Yenisey	Qin	2909158 (GRDC)	1911–1999	Scaled Up	
s	Vilyuyeskoye	Tuba	Qin	2909314 (GRDC)	1941–1989	Scaled Up	
		Total Inflow	Qin	Synthetic	1989–2010	N/A	
		N/A	WSL	0434 (G-REALM)	1992–2019	Unaltered	—
		Vilyuy	Qout	2903703 (GRDC)	1959–1994	Scaled Down	
		Batyr	Qin	2903750 (GRDC)	1970–1994	Scaled Up	
		Churkuo	Qin	2903745 (GRDC)	1971–1992	Scaled Up	
		Vilyuy	Qin	2903704 (GRDC)	1965–2015	Scaled Up	
		Total Inflow	Qin	Synthetic	1994–2010	N/A	

**Table A2**

A-HYPE governing equations. Equation numbers correspond to Fig. 2. Symbol “φ” indicates a parameter derived using the Reservoir Analysis Tool (RAT), with derivation from historic records summarized in Table A3.

#	Where	Equation
A-49	No Conditions	$WSL_{i+1} = WSL_i + \frac{86400 \times (\sum Q_{in,i} - \sum Q_{out,i})}{SA \times 10^6} + \frac{(P_i - ET_i)}{10^3}$
A-50	No Conditions	$Q_{default} = \frac{(\phi_{WSL,ref} - \phi_{WSL,min}) \times SA \times 10^6}{86400}$
A-51	No Conditions	$Q_{prod,i} = \phi_{prod} \times \left(1 + \phi_{amp} \times \sin\left(\frac{2\pi \times (DOY_i + \phi_{phase})}{365}\right)\right)$
A-52	No Conditions	$Q_{econ,i} = Q_{prod,i} \times \frac{(WSL_i - \phi_{WSL,lim})}{(\phi_{WSL,lim} - \phi_{WSL,min})}$
A-53	No Conditions	$Q_{spill,i} = \phi_{rate} \times (WSL_i - \phi_{WSL,ref})^{\phi_{exp}}$
A-54	$WSL_i \leq \phi_{WSL,min}, Q_{prod,i} < Q_{econ,i}$	$Q_{out,i} = Q_{prod,i}$
A-55	$WSL_i \leq \phi_{WSL,min}, Q_{prod,i} > Q_{econ,i}$	$Q_{out,i} = Q_{econ,i}$
A-56	$\phi_{wsL,min} \leq WSL_i \leq \phi_{WSL,ref}, Q_{prod,i} > Q_{default,i}$	$Q_{out,i} = Q_{default,i}$
A-57	$\phi_{wsL,min} \leq WSL_i \leq \phi_{WSL,ref}, Q_{prod,i} < Q_{default,i}$	$Q_{out,i} = Q_{prod,i}$
A-58	$WSL_i > \phi_{WSL,ref}, Q_{prod,i} < Q_{spill,i}$	$Q_{out,i} = Q_{prod,i}$
A-59	$WSL_i > \phi_{WSL,ref}, Q_{prod,i} > Q_{spill,i}$	$Q_{out,i} = Q_{spill,i}$

These equations summarize the outflow and WSL computations used for hydroelectric reservoirs in HYPE (“Rivers and Lakes”, 2020). Equation A-49 computes the daily level as in A-7. Equation 50 computes the default outflow for a regulated reservoir ( $Q_{default}$ ) is the equivalent volume between the minimum

and spillway depths ( $\varphi_{WSL,min}$  and  $\varphi_{WSL,ref}$ ) for a single timestep. Equation 51 computes the daily production zone target outflow ( $Q_{prod,i}$ ) based on the current day-of-year (DOY<sub>i</sub>) and three parameters defining a sine curve ( $\varphi_{prod}$ ,  $\varphi_{amp}$ , and  $\varphi_{phase}$ ). Equation 52 computes the daily storage economizing outflow ( $Q_{econ,i}$ ) by linear interpolation below a threshold ( $\varphi_{WSL,lim}$ ). Equation 53 computes daily outflow representative of a spillway ( $Q_{spill,i}$ ) based on daily WSL (WSL<sub>i</sub>), the depth above the dam top ( $\varphi_{WSL,ref}$ ), and two parameters computed by log10 least squares regression ( $\varphi_{rate}$  and  $\varphi_{exp}$ ). Equations A-54 through A-59 determine the current timestep's outflow based on the current lake depth and relative values of outflow ( $Q_{econ,i}$ ,  $Q_{default,i}$ ,  $Q_{prod,i}$ , and  $Q_{spill,i}$ ).

#	Where	Equation
A-60	No Conditions	$Q_{threshold1} = \frac{(\varphi_{Qmain,max} - \varphi_{Qmain,min})}{\varphi_{fraction}} + \varphi_{Qmain,min}$
A-61	No Conditions	$Q_{threshold2} = \frac{\varphi_{Qbr,max}}{(1 - \varphi_{fraction})} + \varphi_{Qmain,min}$
A-62	No Conditions	$Q_{threshold} = MAX(Q_{threshold1}, Q_{threshold2}, 0)$
A-63	No Conditions	$Q_{total,i} = Q_{out,i}$
A-64	$Q_{total,i} \leq \varphi_{Qmain,min}$	$Q_{out,i} = Q_{total,i}$
A-65	$\varphi_{Qmain,min} < Q_{total,i} \leq Q_{threshold}$	$Q_{out,i} = (Q_{total,i} - \varphi_{Qmain,min}) \times \varphi_{fraction} + \varphi_{Qmain,min}$
A-66	$Q_{threshold} > Q_{total,i}$ , $Q_{threshold} = Q_{threshold1}$	$Q_{out,i} = \varphi_{Qmain,max}$
A-67	$Q_{threshold} > Q_{total,i}$ , $Q_{threshold} = Q_{threshold2}$	$Q_{out,i} = Q_{total,i} - \varphi_{Qbr,max}$
A-68	No Conditions	$Q_{br,i} = Q_{total,i} - Q_{out,i}$

Equations A-60 through A-68 are only computed where a second outlet exists. Equations A-60, A-61, and A-62 compute the threshold main outlet outflow ( $Q_{threshold}$ ) based on the available parameters. Equation A-64 computes the daily main outlet outflow when the total available outflow is less than the threshold. Equation A-65 computes main outlet outflow based on two parameters: the minimum main outlet outflow ( $\varphi_{Qmain,min}$ ) and the fraction of outflow devoted to main outlet ( $\varphi_{fraction}$ ). Equation A-66 computes main outlet outflow where a maximum main outlet outflow parameter has been defined ( $\varphi_{Qmain,max}$ ). Equation A-67 computes main outlet outflow where a maximum secondary outlet outflow parameter has been defined ( $\varphi_{Qbr,max}$ ). Equation A-68 computes secondary outlet outflow ( $Q_{br,i}$ ) based on the new main outlet outflow ( $Q_{out,i}$ ) and total available daily outflow ( $Q_{total,i}$ ). Main and secondary outlet outflow are used to compute the next timestep's WSL (Equation A-49).

## References

- Adeloye, A.J., Soundharajan, B.-S., Ojha, C.S.P., Remesan, R., 2015. Effect of hedging integrated rule curves on the performance of the Pong Reservoir (India) during scenario-neutral climate change perturbations. Water Resour. Manag. 30 (2), 445–470. <https://doi.org/10.1007/s11269-015-1171-z>.
- Ahn, J.M., Lee, S., Kang, T., 2014. Evaluation of dams and weirs operating for water resource management of the Geum River. Sci. Total Environ. 478, 103–115. <https://doi.org/10.1016/j.scitotenv.2014.01.038>.
- Alvarez, H.U.F., Trudel, M., Leconte, R., 2014. Impacts and adaptation to climate change using a reservoir management tool to a northern watershed: application to Lièvre River watershed, Québec, Canada. Water Resour. Manag. 28 (11), 3667–3680. <https://doi.org/10.1007/s11269-014-0694-z>.
- Amir Jabbari, A., Nazemi, A., 2019. Alterations in Canadian hydropower production potential due to continuation of historical trends in climate variables. Resources 8 (4), 163. <https://doi.org/10.3390/resources8040163>.
- Andersson, J., Pechlivanidis, I., Gustafsson, D., Donnelly, C., Arheimer, B., 2015. Key factors for improving large-scale hydrological model performance. European Water 49, 77–88.
- Arheimer, B., Donnelly, C., Lindstrom, G., 2017. Regulation of snow-fed rivers affects flow regimes more than climate change. Nat. Commun. 8 (1), 62. <https://doi.org/10.1038/s41467-017-0009-8>.
- Arheimer, B., Pimentel, R., Isberg, K., Crochmore, L., Andersson, J., Hasan, A., Pineda, L., 2020. Global catchment modelling using World-Wide HYPE (WWH), open data, and stepwise parameter estimation. Hydrol. Earth Syst. Sci. 24 (2), 535–559. <https://doi.org/10.5194/hess-24-535-2020>.
- Asadzadeh, M., Razavi, S., Tolson, B.A., Fay, D., 2014. Pre-emption strategies for efficient multi-objective optimization: application to the development of Lake Superior regulation plan. Environ. Model. Software 54, 128–141. <https://doi.org/10.1016/j.envsoft.2014.01.005>.
- Barber, D.G., 2014. BaySys – contributions of climate change and hydroelectric regulation to the variability and change of freshwater-marine coupling in the Hudson Bay System. Retrieved from (5 November 2017). [http://umanitoba.ca/faculties/environment/departments/ceos/media/BaySys\\_PROJECT\\_DESCRIPTION.pdf](http://umanitoba.ca/faculties/environment/departments/ceos/media/BaySys_PROJECT_DESCRIPTION.pdf).
- Bellin, A., Majone, B., Cainelli, O., Alberici, D., Villa, F., 2016. A continuous hydrological and water resources management model. Environ. Model. Software 75, 176–192. <https://doi.org/10.1016/j.envsoft.2015.10.013>.
- Berg, P., Donnelly, C., Gustafsson, D., 2018. Near-real-time adjusted reanalysis forcing data for hydrology. Hydrol. Earth Syst. Sci. 22 (2), 989–1000. <https://doi.org/10.5194/hess-22-989-2018>.
- Bergstrand, M., Asp, S.S., Lindstrom, G., 2013. Nationwide hydrological statistics for Sweden with high resolution using the hydrological model S-HYPE. Nord. Hydrol. 45 (3), 349–356. <https://doi.org/10.2166/nh.2013.010>.
- Beven, K., 2012. Causal models as multiple working hypotheses about environmental processes. Compt. Rendus Geosci. 344 (2), 77–88. <https://doi.org/10.1016/j.crte.2012.01.005>.
- Cheng, C.T., Chau, K.W., 2004. Flood control management system for reservoirs. Environ. Model. Software 19 (12), 1141–1150. <https://doi.org/10.1016/j.envsoft.2003.12.004>.
- Coerver, H.M., Rutten, M.M., van de Giesen, N.C., 2018. Deduction of reservoir operating rules for application in global hydrological models. Hydrol. Earth Syst. Sci. 22 (1), 831–851. <https://doi.org/10.5194/hess-22-831-2018>.
- Crate, S.A., 2002. Co-option in Siberia: the case of diamonds and the vilyuy sakha. Polar Geogr. 26 (4), 289–307. <https://doi.org/10.1080/789610151>.
- Denaro, S., Anghileri, D., Giuliani, M., Castelletti, A., 2017. Informing the operations of water reservoirs over multiple temporal scales by direct use of hydro-meteorological data. Adv. Water Resour. 103, 51–63. <https://doi.org/10.1016/j.advwatres.2017.02.012>.
- Déry, S.J., Stieglitz, M., McKenna, E.C., Wood, E.F., 2005. Characteristics and trends of river discharge into Hudson, James and Ungava bays, 1964–2000. J. Clim. 18 (14), 2540–2557. <https://doi.org/10.1175/JCLI3440.1>.
- Déry, S.J., Hernández-Henríquez, M.A., Burford, J.E., Wood, E.F., 2009. Observational evidence of an intensifying hydrological cycle in northern Canada. Geophys. Res. Lett. 36 (13), L13402. <https://doi.org/10.1029/2009GL038852>.
- Déry, S.J., Mlynowski, T.J., Hernández-Henríquez, M.A., Straneo, F., 2011. Interannual variability and interdecadal trends in Hudson Bay streamflow. J. Mar. Syst. 88 (3), 341–351. <https://doi.org/10.1016/j.jmarsys.2010.12.002>.
- Déry, S.J., Stadnyk, T.A., MacDonald, M.K., Gauli-Sharma, B., 2016. Recent trends and variability in river discharge across northern Canada. Hydrol. Earth Syst. Sci. 20 (12), 4801–4818. <https://doi.org/10.5194/hess-2016-461>.
- Déry, S.J., Stadnyk, T.A., MacDonald, M.K., Koenig, K.A., Guay, C., 2018. Flow alteration impacts on Hudson Bay river discharge. Hydrol. Process. 32 (24), 3576–3587. <https://doi.org/10.1002/hyp.13285>.
- Donnelly, C., Yang, W., Dahné, J., 2014. River discharge to the Baltic Sea in a future climate. Climatic Change 122 (1–2), 157–170. <https://doi.org/10.1007/s10584-013-0941-y>.
- Donnelly, C., Andersson, J.C., Arheimer, B., 2016. Using flow signatures and catchment similarities to evaluate the E-HYPE multi-basin model across Europe. Hydrol. Sci. J. 61 (2), 255–273. <https://doi.org/10.1080/02626667.2015.1027710>.
- Ehsani, N., Fekete, B.M., Vörösmarty, C.J., Tessler, Z.D., 2016. A neural network based general reservoir operation scheme. Stoch. Environ. Res. Risk Assess. 30 (4), 1151–1166. <https://doi.org/10.1007/s00477-015-1147-9>.
- Global Runoff Data Centre (GRDC), 2020. Monthly data of the 560 stations Arctic-HYCOS basic network available at. [https://www.bafg.de/GRDC/EN/04\\_spcltdbss/41\\_ARDB/ArcticHYCOSData.html?nn=201698](https://www.bafg.de/GRDC/EN/04_spcltdbss/41_ARDB/ArcticHYCOSData.html?nn=201698), accessed May 2020.
- Grill, G., Lehner, B., Lumsdon, A.E., MacDonald, G.K., Zarfl, C., Liermann, C.R., 2015. An index-based framework for assessing patterns and trends in river fragmentation and flow regulation by global dams at multiple scales. Environ. Res. Lett. 10, L015001. <https://doi.org/10.1088/1748-9326/10/1/015001>.
- Gupta, H.V., Kling, H., Yilmaz, K.K., Martinez, G.F., 2009. Decomposition of the mean squared error and NSE performance criteria: implications for improving hydrological modelling. J. Hydrol. 377 (1–2), 80–91. <https://doi.org/10.1016/j.jhydrol.2009.08.003>.

- Haguma, D., Leconte, R., Côté, P., Krau, S., Brissette, F., 2014a. Optimal hydropower generation under climate change conditions for a northern water resources system. *Water Resour. Manag.* 28 (13), 4631–4644. <https://doi.org/10.1007/s11269-014-0763-3>.
- Haguma, D., Leconte, R., Krau, S., Côté, P., Brissette, F., 2014b. Water resources optimization method in the context of climate change. *J. Water Resour. Plann. Manag.* 141 (2), 04014051 [https://doi.org/10.1061/\(ASCE\)WR.1943-5452.0000445](https://doi.org/10.1061/(ASCE)WR.1943-5452.0000445).
- Hanasaki, N., Kanae, S., Oki, T., 2006. A reservoir operation scheme for global river routing models. *J. Hydrol.* 327 (1–2), 22–41. <https://doi.org/10.1016/j.jhydrol.2005.11.011>.
- Hassanzadeh, E., Elshorbagy, A., Wheater, H., Gober, P., 2014. Managing water in complex systems: an integrated water resources model for Saskatchewan, Canada. *Environ. Model. Software* 58, 12–26. <https://doi.org/10.1016/j.envsoft.2014.03.015>.
- Hernández-Henríquez, M.A., Mlynowski, T.J., Déry, S.J., 2010. Reconstructing the natural streamflow of a regulated river: a case study of La Grande Rivière, Québec, Canada. *Can. Water Resour. J.* 35 (3), 301–316. <https://doi.org/10.4296/cwrij3503301>.
- Juston, J.M., Kauffeldt, A., Quesada Montano, B., Seibert, J., Beven, K.J., Westerberg, I.K., 2013. Smiling in the rain: seven reasons to be positive about uncertainty in hydrological modelling. *Hydrol. Process.* 27 (7), 1117–1122. <https://doi.org/10.1002/hyp.9625>.
- Kang, D.H., Shi, X., Gao, H., Déry, S.J., 2014. On the changing contribution of snow to the hydrology of the Fraser River Basin, Canada. *J. Hydrometeorol.* 15 (4), 1344–1365. <https://doi.org/10.1175/JHM-D-13-0120.1>.
- Kirchner, J.W., 2006. Getting the right answers for the right reasons: linking measurements, analyses, and models to advance the science of hydrology. *Water Resour. Res.* 42 (3).
- Kourzeneva, E., 2010. External data for lake parameterization in Numerical Weather Prediction and climate modeling. *Boreal Environ. Res.* 15 (2), 165–177.
- Lake of the Woods Control Board – Regulation Guide, 2006. Retrieved from. <http://www.lwcb.ca/reg-guide/rgp-PT1-OVERVIEW.html>. (Accessed 15 October 2018).
- Lehner, B., Döll, P., 2004. Development and validation of a global database of lakes, reservoirs and wetlands. *J. Hydrol.* 296, 1–22. <https://doi.org/10.1016/j.jhydrol.2004.03.028>.
- Lehner, B., Reidy Liermann, C., Revenga, C., Vorosmarty, C., Fekete, B., Crouzet, P., et al., 2016. Global Reservoir and Dam Database, Version 1 (GRanDv1): Dams. <https://doi.org/10.7927/H4N877QK> revision 01.
- Li, L., Xu, H., Chen, X., Simonovic, S.P., 2010. Streamflow forecast and reservoir operation performance assessment under climate change. *Water Resour. Manag.* 24 (1), 83. <https://doi.org/10.1007/s11269-009-9438-x>.
- Lindström, G., Pers, C., Rosberg, J., Strömqvist, J., Arheimer, B., 2010. Development and testing of the HYPE (Hydrological Predictions for the Environment) water quality model for different spatial scales. *Nord. Hydrol.* 41 (3–4), 295–319. <https://doi.org/10.2166/nh.2010.007>.
- Liu, P., Guo, S., Xu, X., Chen, J., 2011. Derivation of aggregation-based joint operating rule curves for cascade hydropower reservoirs. *Water Resour. Manag.* 25 (13), 3177–3200. <https://doi.org/10.1007/s11269-011-9851-9>.
- Malekmohammadi, B., Kerachian, R., Zahraie, B., 2009. Developing monthly operating rules for a cascade system of reservoirs: application of Bayesian networks. *Environ. Model. Software* 24 (12), 1420–1432. <https://doi.org/10.1016/j.envsoft.2009.06.008>.
- Manitoba Hydro, 2010, December 17. Water power act licences: Churchill River diversion final licence request – supporting documentation. Retrieved from (12 September 2018). [https://www.gov.mb.ca/waterstewardship/licensing/crd\\_licence\\_finalization\\_support\\_report.pdf](https://www.gov.mb.ca/waterstewardship/licensing/crd_licence_finalization_support_report.pdf).
- Manitoba Hydro, 2014a. Lake Winnipeg regulation. A document in support of Manitoba hydro's request for a final licence under the Manitoba water power act. July (a), Retrieved from (12 September 2018). [https://www.hydro.mb.ca/regulatory\\_affairs/pdf/lake\\_wpg\\_regulation/lwr\\_complete\\_report.pdf](https://www.hydro.mb.ca/regulatory_affairs/pdf/lake_wpg_regulation/lwr_complete_report.pdf).
- Manitoba Hydro, 2014b. Lake Winnipeg regulation: chapter 2: project licensing, facilities, and operations: how it all works. July (b), Retrieved from (12 September 2018). [https://www.hydro.mb.ca/regulatory\\_affairs/pdf/lake\\_wpg\\_regulation/re\\_port\\_section\\_2.pdf](https://www.hydro.mb.ca/regulatory_affairs/pdf/lake_wpg_regulation/re_port_section_2.pdf).
- Manitoba Hydro, 2014c. Lake Winnipeg regulation: chapter 3: LWR downstream area effects and Manitoba hydro responses. July (c), Retrieved from (12 September 2018). [https://www.hydro.mb.ca/regulatory\\_affairs/pdf/lake\\_wpg\\_regulation/re\\_port\\_section\\_3.pdf](https://www.hydro.mb.ca/regulatory_affairs/pdf/lake_wpg_regulation/re_port_section_3.pdf).
- Manitoba Hydro, 2014d. Lake Winnipeg regulation: Appendix 1: interim license for the regulation of water levels for water power purposes. July (d), Retrieved from (12 September 2018). [https://www.hydro.mb.ca/regulatory\\_affairs/pdf/lake\\_wpg\\_r egulation/Appendix\\_1\\_Interim\\_Water\\_Power\\_Act\\_Licences\\_for\\_LWR\\_and\\_Jenpeg.pdf](https://www.hydro.mb.ca/regulatory_affairs/pdf/lake_wpg_r egulation/Appendix_1_Interim_Water_Power_Act_Licences_for_LWR_and_Jenpeg.pdf).
- Manitoba Hydro, 2014e. Lake Winnipeg regulation: Appendix 3: an assessment of Lake Winnipeg regulation effects based on hydrometric data. July (e), Retrieved from (12 September 2018). [https://www.hydro.mb.ca/regulatory\\_affairs/pdf/lake\\_wpg\\_reg ulation/Appendix\\_3\\_An\\_Assessment\\_of\\_LWR\\_Effects\\_Based\\_on\\_Hydrometric\\_Data.pdf](https://www.hydro.mb.ca/regulatory_affairs/pdf/lake_wpg_reg ulation/Appendix_3_An_Assessment_of_LWR_Effects_Based_on_Hydrometric_Data.pdf).
- Manitoba Hydro, 2014f. Lake Winnipeg regulation: Appendix 4: an assessment of regulation effects on Lake Winnipeg. July (f), Retrieved from (12 September 2018). [https://www.hydro.mb.ca/regulatory\\_affairs/pdf/lake\\_wpg\\_regulation/Appendix\\_4\\_An\\_Assessment\\_of\\_Regulation\\_Effects\\_on\\_Lake\\_Winnipeg.pdf](https://www.hydro.mb.ca/regulatory_affairs/pdf/lake_wpg_regulation/Appendix_4_An_Assessment_of_Regulation_Effects_on_Lake_Winnipeg.pdf).
- Manitoba Hydro, 2014g. Lake Winnipeg regulation: Appendix 7: lake Winnipeg watershed hydroclimatic study. July (g), Retrieved from (12 September 2018). [https://www.hydro.mb.ca/regulatory\\_affairs/pdf/lake\\_wpg\\_regulation/Appendix\\_7\\_Lake\\_Winnipeg\\_Watershed\\_Hydroclimatic\\_Study.pdf](https://www.hydro.mb.ca/regulatory_affairs/pdf/lake_wpg_regulation/Appendix_7_Lake_Winnipeg_Watershed_Hydroclimatic_Study.pdf).
- Manitoba Hydro, 2015, December 18. Regional cumulative effects assessment for hydroelectric developments on the Churchill, Burntwood and Nelson River systems: integrated summary report. Retrieved from (12 September 2018). [https://www.hydro.mb.ca/regulatory\\_affairs/pdf/rcea/rcea\\_integrated\\_summary.pdf](https://www.hydro.mb.ca/regulatory_affairs/pdf/rcea/rcea_integrated_summary.pdf).
- Matrosov, E.S., Harou, J.J., Loucks, D.P., 2011. A computationally efficient open-source water resource system simulator—Application to London and the Thames Basin. *Environ. Model. Software* 26 (12), 1599–1610. <https://doi.org/10.1016/j.envsoft.2011.07.013>.
- Mehrani, A., Clark, E.A., Lettenmaier, D.P., 2017. Spatial variability of wet troposphere delays over inland water bodies. *J. Geophys. Res.: Atmosphere* 122 (21), 11–329. <https://doi.org/10.1002/2017JD026525>.
- Minville, M., Brissette, F., Krau, S., Leconte, R., 2009a. Adaptation to climate change in the management of a Canadian water-resources system exploited for hydropower. *Water Resour. Manag.* 23 (14), 2965–2986. <https://doi.org/10.1007/s11269-009-9418-1>.
- Minville, M., Brissette, F., Leconte, R., 2009b. Impacts and uncertainty of climate change on water resource management of the Peribonka River System (Canada). *J. Water Resour. Plann. Manag.* 136 (3), 376–385. <https://doi.org/10.1061/ASCE/WR.1943-5452.0000041>.
- Minville, M., Krau, S., Brissette, F., Leconte, R., 2010. Behaviour and performance of a water resource system in Québec (Canada) under adapted operating policies in a climate change context. *Water Resour. Manag.* 24 (7), 1333–1352. <https://doi.org/10.1007/s11269-009-9500-8>.
- Moriasi, Daniel N., et al., 2015. Hydrologic and water quality models: performance measures and evaluation criteria. *Transactions of the ASABE* 58 (6), 1763–1785. <https://doi.org/10.13031/trans.58.10715>.
- Nash, J.E., Sutcliffe, J.V., 1970. River flow forecasting through conceptual models Part I – A discussion of principles. *J. Hydrol.* 10 (3), 282–290. [https://doi.org/10.1016/0022-1694\(70\)90255-6](https://doi.org/10.1016/0022-1694(70)90255-6).
- Nazemi, A., Wheater, H.S., 2015a. On inclusion of water resource management in Earth system models—Part 1: problem definition and representation of water demand. *Hydrol. Earth Syst. Sci.* 19 (1), 33–61. <https://doi.org/10.5194/hess-19-33-2015>.
- Nazemi, A., Wheater, H.S., 2015b. On inclusion of water resource management in Earth system models—Part 2: representation of water supply and allocation and opportunities for improved modeling. *Hydrol. Earth Syst. Sci.* 19 (1), 63–90. <https://doi.org/10.5194/hess-19-63-2015>.
- Nunes, T.H.C., Galvão, C.D.O., Régo, J.C., 2016. Rule curve for seasonal increasing of water concessions in reservoirs with low regularized discharges. *RBRH* 21 (3), 493–501. <https://doi.org/10.1590/2318-0331.011615146>.
- Pechlivanidis, I., Arheimer, B., 2015. Large-scale hydrological modelling by using modified PUB recommendations: the India-HYPE case. *Hydrol. Earth Syst. Sci.* 19 (11), 4559–4579.
- Piman, T., Cochrane, T.A., Arias, M.E., 2016. Effect of proposed large dams on water flows and hydropower production in the Sekong, Sesan and Srepok rivers of the Mekong Basin. *River Res. Appl.* 32 (10), 2095–2108. <https://doi.org/10.1002/rra.3045>.
- Pokhrel, Y., Hanasaki, N., Koirala, S., Cho, J., Yeh, P.-J.-F., Kim, H., Kanae, S., Oki, T., 2012. Incorporating anthropogenic water regulation routines into a land surface model. *J. Hydrometeorol.* 13 (1), 255–269.
- Prasanchum, H., Kangrang, A., 2018. Optimal reservoir rule curves under climatic and land use changes for Lampang Dam using Genetic Algorithm. *KSCJ. J. Civ. Eng.* 22 (1), 351–364. <https://doi.org/10.1007/s12205-017-0676-9>.
- Processes above ground [HYPE model documentation]. Retrieved from (01 September 2020). [http://www.smhi.net/hype/wiki/doku.php?id=start:hype\\_model\\_descriptio n:processes\\_above\\_ground](http://www.smhi.net/hype/wiki/doku.php?id=start:hype_model_descriptio n:processes_above_ground).
- Province of Manitoba, 1973, May. Water power act: interim license for the diversion of water from the Churchill River to the Nelson River, and the impoundment of water on the Rat River and southern Indian lake. Retrieved from (12 September 2018). [https://www.gov.mb.ca/waterstewardship/licensing/pdf/crd\\_may73.pdf](https://www.gov.mb.ca/waterstewardship/licensing/pdf/crd_may73.pdf).
- Province of Manitoba, 1975. Final licence for the development of water power: Grand Rapids site, Saskatchewan River. Retrieved from (12 September 2018). [https://www.gov.mb.ca/waterstewardship/licensing/pdf/grand\\_rapids/grand\\_rapids\\_1975.pdf](https://www.gov.mb.ca/waterstewardship/licensing/pdf/grand_rapids/grand_rapids_1975.pdf).
- Province of Manitoba, 2018. Water power act: CRD augmented flow program. Retrieved from (12 September 2018). [https://www.gov.mb.ca/waterstewardship/licensing/pdf/augmented\\_flow\\_program\\_2018.pdf](https://www.gov.mb.ca/waterstewardship/licensing/pdf/augmented_flow_program_2018.pdf).
- Qin, Y., Mueller, N.D., Siebert, S., Jackson, R.B., AghaKouchak, A., Zimmerman, J.B., et al., 2019. Flexibility and intensity of global water use. *Nature Sustainability* 1. <https://doi.org/10.1038/s41893-019-0294-2>.
- Revilla-Romero, B., Wanders, N., Burek, P., Salamon, P., de Roo, A., 2016. Integrating remotely sensed surface water extent into continental scale hydrology. *J. Hydrol.* 543, 659–670. <https://doi.org/10.1016/j.jhydrol.2016.10.041>.
- River and lakes [HYPE model documentation]. Retrieved from (01 September 2020). [http://www.smhi.net/hype/wiki/doku.php?id=start:hype\\_model\\_description:h ype\\_routing](http://www.smhi.net/hype/wiki/doku.php?id=start:hype_model_description:h ype_routing).
- Shin, S., Pokhrel, Y., Miguez-Macho, G., 2019. High-resolution modeling of reservoir release and storage dynamics at the continental scale. *Water Resour. Res.* 55 (1), 787–810. <https://doi.org/10.1029/2018WR023025>.
- Shook, K., Pomeroy, J.W., 2016. The effects of the management of Lake Diefenbaker on downstream flooding. *Canadian Water Resources Journal/Revue canadienne des ressources hydrauliques* 41 (1–2), 261–272. <https://doi.org/10.1080/07011784.2015.1092887>.
- Solander, K.C., Reager, J.T., Thomas, B.F., David, C.H., Famiglietti, J.S., 2016. Simulating human water regulation: the development of an optimal complexity,

- climate-adaptive reservoir management model for an LSM. *J. Hydrometeorol.* 17 (3), 725–744. <https://doi.org/10.1175/JHM-D-15-0056.1>.
- Stadnyk, T.A., Déry, S.J., MacDonald, M.K., Koenig, K.A., 2019. Theme 1: physical environment. Iv. The freshwater system. In: Kuzyk, Z.A., Candlish, L.M. (Eds.), From Science to Policy in the Greater Hudson Bay: an Integrated Regional Impact Study (IRIS) of Climate Change and Modernization, pp. 113–155. ArcticNet.
- Stadnyk, T.A., MacDonald, M.K., Tefs, A., Awoye, O.H.R., Déry, S.J., Gustafsson, D., Isberg, K., Arheimer, B., 2020. Hydrological modeling of freshwater discharge into Hudson Bay using HYPE, 8. Elementa: Science of the Anthropocene.
- Taghian, M., Rosbjerg, D., Haghghi, A., Madsen, H., 2013. Optimization of conventional rule curves coupled with hedging rules for reservoir operation. *J. Water Resour. Plann. Manag.* 140 (5), 693–698. [https://doi.org/10.1061/\(ASCE\)WR.1943-5452.0000355](https://doi.org/10.1061/(ASCE)WR.1943-5452.0000355).
- Tyaptiryanov, M.M., Tyaptiryanova, V.M., 2016. Quality standard of the water, environment, and hydrobiota in the River Vilyuy basin. *Yakut Medical Journal* (3), 98–102.
- United States Department of Agriculture's Foreign Agricultural Service (USDA-FAS), 2020. Global reservoirs and lakes monitor (G-REALM). United states department of agriculture's. Retrieved from (13 June 2020). [https://ipad.fas.usda.gov/crope\\_xplorer/global\\_reservoir/](https://ipad.fas.usda.gov/crope_xplorer/global_reservoir/).
- Wada, Y., Bierkens, M.F., Roo, A.D., Dirmeyer, P.A., Famiglietti, J.S., Hanasaki, N., et al., 2017. Human–water interface in hydrological modelling: current status and future directions. *Hydrol. Earth Syst. Sci.* 21 (8), 4169–4193. <https://doi.org/10.5194/hess-21-4169-2017>.
- Wanders, N., Wada, Y., 2015. Human and climate impacts on the 21st century hydrological drought. *J. Hydrol.* 526, 208–220. <https://doi.org/10.1016/j.jhydrol.2014.10.047>.
- Water Survey of Canada (WSC), 2020. Water Survey of Canada. Environment Canada, Ottawa. Retrieved from (15 August 2020). [https://wateroffice.ec.gc.ca/mainmenu/historical\\_data\\_index\\_e.html](https://wateroffice.ec.gc.ca/mainmenu/historical_data_index_e.html).
- Welsh, W.D., Vaze, J., Dutta, D., Rassam, D., Rahman, J.M., Jolly, I.D., et al., 2013. An integrated modelling framework for regulated river systems. *Environ. Model. Software* 39, 81–102. <https://doi.org/10.1016/j.envsoft.2012.02.022>.
- Wu, Y., Chen, J., 2012. An operation-based scheme for a multiyear and multipurpose reservoir to enhance macroscale hydrologic models. *J. Hydrometeorol.* 13 (1), 270–283. <https://doi.org/10.1175/JHM-D-10-05028.1>.
- Yassin, F., Razavi, S., Elshamy, M., Davison, B., Saprizia-Azuri, G., Wheater, H., 2019. Representation and improved parameterization of reservoir operation in hydrological and land-surface models. *Hydrol. Earth Syst. Sci.* 23 (9), 3735–3764. <https://doi.org/10.5194/hess-23-3735-2019>.
- Zaherpour, J., Gosling, S.N., Mount, N., Schmied, H.M., Veldkamp, T.I., Dankers, R., et al., 2018. Worldwide evaluation of mean and extreme runoff from six global-scale hydrological models that account for human impacts. *Environ. Res. Lett.* 13 (6), 065015 <https://doi.org/10.1088/1748-9326/aac547>.
- Zajac, Z., Revilla-Romero, B., Salamon, P., Burek, P., Hirpa, F.A., Beck, H., 2017. The impact of lake and reservoir parameterization on global streamflow simulation. *J. Hydrol.* 548, 552–568. <https://doi.org/10.1016/j.jhydrol.2017.03.022>.
- Zhang, W., Liu, P., Wang, H., Chen, J., Lei, X., Feng, M., 2017. Reservoir adaptive operating rules based on both of historical streamflow and future projections. *J. Hydrol.* 553, 691–707. <https://doi.org/10.1016/j.jhydrol.2017.08.031>.
- Zhao, G., Gao, H., Naz, B.S., Kao, S.C., Voisin, N., 2016. Integrating a reservoir regulation scheme into a spatially distributed hydrological model. *Adv. Water Resour.* 98, 16–31. <https://doi.org/10.1016/j.advwatres.2016.10.014>.
- Zhou, Y., Guo, S., 2013. Incorporating ecological requirement into multipurpose reservoir operating rule curves for adaptation to climate change. *J. Hydrol.* 498, 153–164. <https://doi.org/10.1016/j.jhydrol.2013.06.028>.